THE JOURNAL
OF
CHEMICAL PHYSICS

VOLUME 12, NUMBER 7 JULY, 1944

The Effect of Substituents on the Dissociation Constants of Carboxylic Acids

JAMES N. SARMOUSAKIS*
Department of Chemistry and Chemical Engineering, University of Pennsylvania, Philadelphia, Pennsylvania
(Received April 24, 1944)

The Kirkwood-Westheimer electrostatic theory for relative acid strength has been extended by the use of an oblate spheroidal molecular model and applied to the study of a number of substituted benzoic acids. When reasonable values of certain structural and electrical parameters, describing the acid and base molecules in equilibrium, are used, the agreement between theory and experiment with respect to the meta acids is good. The theoretically calculated and experimentally determined values of log $K_{A_xB_0}$ for the parasubstituted acids, where $K_{A_xB_0}$ is the ratio of the dissociation constant of the substituted acid to that of the parent acid, show differences $\Delta \log K_{A_xB_0}$ which may be considered measures of the resonance effects operative in the para acids. The quantity $\Delta \log K_{A_xB_0}$ for each acid changes very little from one single-component hydroxylic solvent to another.

PART I. INTRODUCTION AND THEORETICAL RESULTS

A RECENT investigation[1,2] of the acid strengths of the substituted benzoic acids relative to that of benzoic acid in a number of solvents has yielded a quantity of consistent data to which a theory of substituent effects might profitably be applied.

The groundwork for the type of theory to be considered in this paper was laid out by Bjerrum[3] who suggested that a value of the ratio of the first to the second dissociation constant of an uncharged polybasic acid in any solvent might be estimated by taking account of a statistical effect and the influence of the electrostatic field of the negative charge in the acid-ion on the dissociation of a second proton.

Following a similar line of reasoning Waters,[4] Smallwood,[5] Eucken,[6] and Schwarzenbach and Egli[7] came to regard the change of the dissociation constant of an organic acid due to the substitution of a polar group as largely connected with the electrostatic interaction of an electric dipole, representing the group, with the dissociating proton. In their calculations of electrostatic interaction energies, the three last mentioned authors took cognizance of the low electric polarizability within a molecule by using effective dielectric constants having values between that of the dielectric constant of the solvent and that which the molecules may be presumed to have.

By characterizing the molecules of the related acids and their conjugate bases[8] as sets of charges embedded in equal cavities of low dielectric con-

* Now at the Ballistic Research Laboratory, Aberdeen Proving Ground, Maryland.

[1] J. H. Elliott and M. Kilpatrick, J. Phys. Chem. **45**, 454, 466, 472, 485 (1941).

[2] J. H. Elliott, J. Phys. Chem. **46**, 221 (1942).

[3] N. Bjerrum, Zeits. f. physik. Chemie **106**, 219 (1923).

[4] W. A. Waters, Phil. Mag. **8**, 436 (1929).

[5] H. M. Smallwood, J. Am. Chem. Soc. **54**, 3048 (1932).

[6] A. Eucken, Zeits. f. angew. Chemie **45**, 203 (1932).

[7] G. Schwarzenbach and H. Egli, Helv. Chim. Acta **17**, 1183 (1934).

[8] M. Kilpatrick, Chem. Rev. **30**, 159 (1942).

stant in a continuous solvent medium of high dielectric constant, Kirkwood and Westheimer[9,10] also developed relations between the first two dissociation constants of a polybasic acid and between the dissociation constants of a substituted acid and its unsubstituted parent acid. Their equations, which are similar in form to those of their predecessors in the field, contain an effective dielectric constant which is an explicit function of the dielectric constants of the solvent and the molecular cavities, the distance between the dissociating protons or between dissociating proton and substituent dipole, as the case may be, and of the parameter defining the shape of the cavity.

Two molecular models were set up featuring spherical[9] and prolate spheroidal[10] cavities. The theoretical results were applied to the aliphatic acids[9–11] with considerable success. In the field of benzenoid compounds the theory was applied[12] to experimental data only for the parasubstituted monobasic and the paradibasic acids. Due to resonance effects[13] the application of such a purely electrostatic theory to these acids alone was of limited usefulness.

In the case of the meta benzenoid acids, however, substituent effects have hitherto been considered to be but little complicated by resonance phenomena.[13] Accordingly a theory of the Kirkwood-Westheimer type should probably apply best to this class of acids and should yield information which would be useful in appraising the contributions of the various factors which affect the acid strengths of the para isomers. It is the program of this paper to develop and use such a theory in this manner.

The development follows that of Kirkwood and Westheimer in all fundamentals. There is considered the reaction, $A_1+B_2\rightleftarrows A_2+B_1$, with equilibrium constant[8] $K_{A_1B_2}$ where A_1 and A_2 are benzenoid acid molecules and B_1 and B_2 their conjugate bases. A_1 and A_2 are described as having point charge configurations identical in every respect except that A_1 possesses a number of charges in excess of A_2. The excess charges reduce to the first dissociating proton, if A_1 is a polybasic acid, or to a point dipole, if A_1 is a substituted acid. The two charge configurations are assumed to lie in cavities of the same shape, size, and internal dielectric constant placed in a continuous medium with a high dielectric constant equal to that of the solvent. The conjugate base molecules B_1 and B_2 are assumed to be formed from A_1 and A_2 by the dissociation of protons without further change in the acid molecules.

With the well-known flat ring structure of benzenoid molecules in mind, it is reasonable to assume the cavities just considered to be oblate spheroids with their charges on the focal disks and all dissociating protons and substituent dipoles on the focal circles. Calculations with this model are facilitated by the use of the oblate spheroidal coordinates ζ, η, and, ϕ, which are defined in terms of Cartesian coordinates x, y,and z by the equations:

$$\begin{aligned} x&=c(1+\zeta^2)^{\frac{1}{2}}(1-\eta^2)^{\frac{1}{2}}\cos\phi,\\ y&=c(1+\zeta^2)^{\frac{1}{2}}(1-\eta^2)^{\frac{1}{2}}\sin\phi, \qquad (1)\\ z&=c\eta\zeta. \end{aligned}$$

The parameters ζ, η, and ϕ define orthogonal families of oblate spheroids, hyperboloids of one sheet, and half-planes, respectively. The focal ring of the spheroids and hyperboloids has the radius c.

The equilibrium constant, $K_{A_1B_2}$, is then to be approximated by means of the relations

$$2.303kT\log(K_{A_1B_2}/\sigma)=\Delta W \qquad (2)$$

and

$$\Delta W=W(A_1)+W(B_2)-W(A_2)-W(B_1),$$

where σ is the statistical factor and $W(A_1)$, $W(A_2)$, $W(B_1)$, and $W(B_2)$ each represent the electrostatic work of formation of the corresponding molecule in the solvent. The quantities W and ΔW may be calculated by the use of expressions for the electrostatic potential obtained by the solution of Laplace's equation in the coordinates ζ, η, and ϕ. The calculations are outlined in Part IV of this paper.

[9] J. G. Kirkwood and F. H. Westheimer, J. Chem. Phys. 6, 506 (1938).
[10] F. H. Westheimer and J. G. Kirkwood, J. Chem. Phys. 6, 513 (1938).
[11] F. H. Westheimer and M. W. Shookhoff, J. Am. Chem. Soc. 61, 555 (1939).
[12] F. H. Westheimer, J. Am. Chem. Soc. 61, 1977 (1939).
[13] G. E. K. Branch and M. Calvin, *The Theory of Organic Chemistry* (Prentice-Hall, Inc., New York, 1941).

For the ratio of the first to the second dissociation constants of a polybasic acid, the considerations of Part IV lead to the following relation which is similar in form to that of Bjerrum,[3]

$$\log [K_1/(K_2\sigma)] = e^2/(2.303kTrD_E),$$

where

$$\frac{1}{D_E} = \frac{1}{D_i} + \left(\frac{1}{D} - \frac{1}{D_i}\right) \times \sum_{\substack{n=0 \\ (n+m)\text{ even}}}^{\infty} \sum_{m=0}^{n} \frac{r}{c} \frac{\alpha_n^m}{1-(D_i/D)Y_n^m} \cos m\Phi, \tag{3}$$

$$\alpha_n^m = i(2-\delta_m^0)(2n+1) \times \frac{[(n-m)!(n+m)!]^2}{\left[2^n\left(\frac{n-m}{2}\right)!\left(\frac{n+m}{2}\right)!\right]^4} \frac{Q_n^m(i\zeta_0)}{P_n^m(i\zeta_0)},$$

TABLE I. f_1 and f_2 for dibasic acids.

	Ortho		Meta		Para	
ζ_0	f_1	f_2	f_1	f_2	f_1	f_2
0.4					0.00004	0.85986
0.5					0.00044	0.75598
0.6					0.00192	0.74652
0.7	0.0380	0.9096	0.0081	0.7815	0.0056	0.7454
0.8	0.0674	0.9028	0.0177	0.7862	0.0118	0.7492
0.9	0.1038	0.8850	0.0304	0.7914	0.0214	0.7544
1.0	0.1446	0.8578	0.0472	0.7933	0.0340	0.7592
1.1	0.1876	0.8240	0.0671	0.7930	0.0492	0.7618
1.2	0.2306	0.7867	0.0894	0.7867	0.0670	0.7618
1.3	0.2724	0.7480	0.1133	0.7782	0.0862	0.7594
1.4	0.3121	0.7096	0.1385	0.7670	0.1072	0.7542
1.6	0.3842	0.6379	0.1897	0.7382	0.1504	0.7362
1.8	0.4467	0.5733	0.2398	0.7048	0.1946	0.7152
2.0	0.4978	0.5185	0.2872	0.6696	0.2376	0.6896
2.2	0.5418	0.4720	0.3401	0.6260	0.2788	0.6618
2.4	0.5793	0.4323	0.3718	0.6012	0.3172	0.6338

and

$$Y_n^m = \frac{m\zeta_0 + (1+\zeta_0^2)^{\frac{1}{2}} P_n^{m+1}(i\zeta_0)/P_n^m(i\zeta_0)}{m\zeta_0 + (1+\zeta_0^2)^{\frac{1}{2}} Q_n^{m+1}(i\zeta_0)/Q_n^m(i\zeta_0)}.$$

In this relation K_1 and K_2 are the first and second dissociation constants of the polybasic acid, and σ is a statistical factor equal to four for symmetric dibasic acids and three for symmetric tribasic acids and their primary acid-ions. e is the protonic charge, k is Boltzmann's constant, T is the absolute temperature, r is the distance between the dissociating protons, and D_E is the effective dielectric constant. D_i and D are the dielectric constants of the molecular cavities and the solvent, respectively, and Φ is the angle between the radii of the focal circle to the dissociating protons. The quantity r/c takes on the values 1, $\sqrt{3}$, and 2 and the quantity Φ the values 60°, 120°, and 180° for ortho, meta, and para (dibasic or substituted monobasic) acids, respectively. δ_m^0 equals zero when $m \neq 0$ or unity when $m = 0$. The parameter ζ_0 defines the molecular cavity. $P_n^m(i\zeta_0)$ and $Q_n^m(i\zeta_0)$ are associated Legendre functions of the first and second kind, respectively, defined for imaginary variable.[14]

Correspondingly, the ratio[8] $K_{A_xB_0}$ of the dissociation constant of the acid A_x, obtained by substituting the polar group X in a parent benzenoid acid A_0, to that of the acid A_0 is given by the equation,

$$\log K_{A_xB_0} = \frac{1}{2.303kT}\left[-\frac{e(\mathfrak{y}, \mathbf{r})}{D_i r^3} + \left(\frac{1}{D} - \frac{1}{D_i}\right) \sum_{\substack{n=0 \\ (n+m)\text{ even}}}^{\infty} \sum_{m=0}^{n} \frac{\alpha_n^m}{1-(D_i/D)Y_n^m} \frac{e}{c^2} \times \mathfrak{y}\{\mathbf{i}_1(n^2-m^2+n)\cos m\Phi - \mathbf{i}_2 m \sin m\Phi\}\right], \tag{4}$$

where r is the length of the line vector $\mathbf{r}$ from the dissociating proton to the substituent dipole of moment $\mathfrak{y}$. The moment $\mathfrak{y}$ equals the difference between the group moment of the substituent X and that of the hydrogen atom replaced and its direction is that of the motion of a small positive charge placed on the dipole axis. The unit vector $\mathbf{i}_1$ is directed from the center of the focal circle along the radius to the dipole $\mathfrak{y}$ and makes an angle Φ with the radius to the dissociating proton, whereas $\mathbf{i}_2$ is the corresponding unit vector tangent to the focal circle in the direction of increasing ϕ. The other symbols are as in Eq. (3).

Expansion of the quantity $[1-(D_i/D)Y_n^m]^{-1}$ in a binominal series, followed by rejection of terms in $1/D$ of power higher than the first, makes it possible to convert the formula for $1/D_E$ in Eq. (3) into the form,

$$\frac{1}{D_E} = \frac{f_1}{D_i} + \frac{f_2}{D}. \tag{5}$$

By the summation of the appropriate series the quantities f_1 and f_2 corresponding to ortho, meta,

[14] W. R. Smythe, *Static and Dynamic Electricity* (McGraw-Hill Book Company, Inc., New York, 1939).

and para dibasic acids have been computed for a number of values of ζ_0 and are given in Table I.

The corresponding binomial expansion of $[1-(D_i/D)\,Y_n{}^m]^{-1}$ and rejection of terms in $1/D$ of power higher than the first converts Eq. (4) into the form,

$$\log K_{A_xB_0}=\frac{1}{2.303kT}\left[\frac{-e|\mu_\zeta|\cos(\mu_\zeta \mathbf{i}_1,\mathbf{r})}{r^2D_\zeta}-\frac{e|\mu_\phi|\cos(\mu_\phi \mathbf{i}_2,\mathbf{r})}{r^2D_\phi}\right], \quad (6)$$

where

$$\frac{1}{D_\zeta}=\frac{g_1}{D_i}+\frac{g_2}{D}, \quad (6a)$$

and

$$\frac{1}{D_\phi}=\frac{h_1}{D_i}+\frac{h_2}{D}, \quad (6b)$$

where μ_ζ and μ_ϕ are the components of the dipole $\boldsymbol{\mu}$ along $\mathbf{i}_1$ and $\mathbf{i}_2$, respectively, and D_ζ and D_ϕ are effective dielectric constants corresponding to the dipole components μ_ζ and μ_ϕ, respectively. Equation (6) in its complete form is required in the treatment of metasubstituted benzenoid acids, while for the para isomers the term due to the dipole component μ_ϕ vanishes. Values of g_1, g_2, h_1, and h_2 for meta acids and g_1 and g_2 for para acids computed for various values of ζ_0 are tabulated in Table II. Values of these functions for ortho acids are not tabulated since the series from which they would be calculated converge too slowly to allow of their summation without considerable labor.

By the use of Eqs. (5), (6), (6a), and (6b) and Tables I and II it may be shown that, as ζ_0 and consequently the volume of the acid molecules with given charge configurations increases, the values of D_E, D_ζ, and D_ϕ approach D_i. Again as ζ_0 approaches zero and the cavity degenerates to a disk, immersing the charges in the solvent, the magnitudes of D_E, D_ζ, and D_ϕ go through values higher than the solvent dielectric constant D. These values must accordingly go through a maximum before becoming equal to D at ζ_0 equal to zero. Again for a given value of ζ_0 and Φ, the value of D_E for dibasic acids is greater than that of D_ζ for substituted acids. Corresponding observations have been noted by Kirkwood and Westheimer[9,10] for their models.

Furthermore it is readily seen that the values of D_E for dibasic acids calculated from the data of Table I for a given value of ζ_0 increase in the order ortho, meta, and para. Similarly the values of D_ζ for metasubstituted acids, computed from Table II, are less than those for the para isomer. These orders of the calculated effective dielectric constants of isomeric benzenoid acid molecules have been suggested by Schwarzenbach.[15] Again for a fixed value of ζ_0 the magnitude of D_ϕ for metasubstituted acids is always greater than D_ζ.

PART II. PARAMETERS AND SAMPLE CALCULATIONS

In this section conventions are adopted for consistently fixing the values of the various parameters appearing in Eqs. (3)–(6), (6a), and (6b). A typical numerical calculation of the type employed in the application to experimental data is also outlined.

TABLE II. g_1, g_2, h_1, and h_2 for substituted acids.

	Meta				Para	
ζ_0	g_1	g_2	h_1	h_2	g_1	g_2
0.4					0.00148	0.8697
0.5					0.00964	0.9103
0.6					0.03112	0.9567
0.7	0.1038	1.0101	0.0334	1.031	0.06844	0.9856
0.8	0.1728	0.9911	0.0640	1.042	0.1192	0.9879
0.9	0.2504	0.9412	0.1042	1.038	0.1792	0.9648
1.0	0.3297	0.8726	0.1546	1.013	0.2432	0.9232
1.1	0.4066	0.7943	0.2086	0.977	0.3088	0.8688
1.2	0.4783	0.7136	0.2650	0.931	0.3716	0.8088
1.3	0.5431	0.6357	0.3232	0.875	0.4312	0.7460
1.4	0.6006	0.5629	0.3790	0.818	0.4864	0.6844
1.6	0.6952	0.4382	0.4828	0.700	0.5828	0.5696
1.8	0.7658	0.3405	0.5728	0.590	0.6612	0.4708
2.0	0.8185	0.2664	0.6472	0.495	0.7232	0.3896
2.2	0.8576	0.2103	0.7084	0.414	0.7728	0.3232
2.4	0.8867	0.1684	0.7574	0.347	0.8124	0.2692

Maximum and intermediate estimates[9] of the proton-proton or proton-dipole distance r for a benzenoid acid may be made by assuming the acid group to be either fully extended or to be executing free internal rotations. For a maximum estimate the dissociating proton is conventionally placed at the projection of its actual position, as calculated by means of x-ray and electron diffraction data, upon the line of the valence bond joining the fully extended acid group to the benzene ring. To obtain the intermediate esti-

[15] G. Schwarzenbach, Helv. Chim. Acta **15**, 1468 (1932).

mate the proton is thought to occupy a mean position in time as the acid group rotates internally. For a halogen substituted acid, the point dipole $\mathfrak{y}$ corresponding to the substituent group is placed at the midpoint of the carbon-halogen bond.[9]

The focal radius c of the oblate spheroidal molecular cavity of a paradibasic or a parasubstituted monobasic benzenoid acid is set equal to $r/2$ and takes on the values c_{Ext} and c_{Rot} depending on whether the carboxyl group is considered fully extended or freely rotating. The values of r for the ortho and meta isomers, whose molecules are assumed to have the same shape and focal radius as those of the para acid, are then set equal to c and $\sqrt{3}c$, respectively. The magnitudes of the distances r for the metahalogenated benzoic acids computed in this way and derived directly from the structural geometry of the molecules differ at most by 0.14A.

Further structural calculations indicate that for metasubstituted benzenoid acids the angles $(\mathfrak{y}, \mathfrak{r})$ do not have the values 150° or 30° required when a dipole is situated on the focal circle 120° from the dissociating proton, and directed along a radius. It has therefore been deemed necessary to assign values of the angles $(\mathfrak{y}, \mathfrak{r})$ to the substituent dipoles of the metahalogenated benzenoid acids calculated from diffraction data assuming the acid groups fully extended. For benzenoid acids with composite substituent groups, whose components are placed farther out from the benzene ring than are those of the halogen, the angles $(\mathfrak{y}, \mathfrak{r})$ have been given rounded values close to those of the corresponding iodosubstituted acid. The resulting components of $\mathfrak{y}$, μ_ξ and μ_ϕ, along the radius and along the tangent of the focal circle, respectively, are easily calculated by trigonometry.

In order to determine a value for the parameter ζ_0 defining the boundary of an oblate spheroidal molecule it is required to estimate not only the focal radius c but also the molecular cavity volume τ which is related to c and ζ_0 by the equation,

$$\tau/c^3 = (4\pi/3)\zeta_0(1+\zeta_0^2). \qquad (7)$$

The molecular cavity of volume τ may be considered to delimit a region of low dielectric constant containing the molecule and a shell of thickness δ roughly corresponding to the relatively empty interstitial space between the molecule itself and the surrounding solvent molecules. Use is made of the concept of van der Waals radii[16] in making estimates of the volumes of the molecules of parasubstituted or unsubstituted benzenoid acids or their conjugate bases which are ellipsoids with axes of different lengths rather than oblate spheroids. The length of the major axis of such an ellipsoid is taken to be equal to the distance between the outermost atoms along the axis of symmetry plus the sum of the van der Waals radii of these atoms. The length of the mean axis is set equal to the distance between the two ortho hydrogen atoms plus twice the van der Waals radius of hydrogen. The length of the minor axis equals the van der Waals thickness of the benzene ring. The ellipsoidal shell around the molecule is assumed arbitrarily to have a thickness δ equal to 0.8A, the average difference between the van der Waals radius and the covalent radius of an atom. The resulting van der Waals volume τ_w including this shell and the molecule within is then considered an approximation to the volume τ of the oblate spheroidal molecular cavity of the present theory. The molecules of the ortho and meta isomers of a para acid or base are assumed to have the same cavity volumes as the molecules of the para compounds. The quantity τ_w as used in the study of relative acid strengths by the electrostatic theory is taken as the average value of τ_w for all four acid and base molecules involved.

To avoid ambiguities concerning the directions of dipole moments, only benzenoid acids with the symmetric substituents NO_2, CN, F, Cl, Br, I, CH_3, and $C(CH_3)_3$ are considered. The values of the dipole moment $|\mathfrak{y}|$, which is the difference between the moment of the substituent group and that of hydrogen, are set equal to the moments of the correspondingly substituted benzenes in the vapor state. For the substituents mentioned they are, in Debyes, respectively, 4.21, 4.39, 1.57, 1.72, 1.70 as given by Smyth,[17] 1.50 as estimated by Groves and Sugden,[18] 0.37 and 0.70

[16] L. Pauling, *The Nature of the Chemical Bond* (Cornell University Press, Ithaca, New York, 1940), second edition.
[17] C. P. Smyth, J. Phys. Chem. **41**, 209 (1937).
[18] L. G. Groves and S. Sugden, J. Chem. Soc., p. 1992 (1937).

as determined by Baker and Groves.[19] The dipole moment vectors for the alkyl groups are directed along radii away from the benzene ring, while those for the other groups mentioned are directed radially into the benzene ring.

D_i has been assigned[9] the value 2.00, while D is the value of the dielectric constant of the solvent medium under consideration. In what follows the values of D for water, glycol, methanol, ethanol, and *n*-propanol are given by Åkerlof,[20] for *n*-butanol by Wooten and Hammett,[21] for dioxane-water mixtures by Åkerlof and Short.[22]

As an illustration of the type of calculation used in applications of the theory, the calculation of log $K_{A_xB_0}$ for *m*-nitrobenzoic acid in water at 25°C is outlined. For this acid τ_w is 255A³, $|\mathfrak{y}|$ is 4.21D, the angle $(\mathfrak{y}, \mathfrak{r})$ is set equal to 140°. c is given the value 3.35A, D_i equals 2.00, and D equals 78.5. From the angle $(\mathfrak{y}, \mathfrak{r})$ it follows that the angles $(\mu_\xi \mathfrak{i}_1, \mathfrak{r})$ and $(\mu_\phi \mathfrak{i}_2, \mathfrak{r})$ are 150° and 60°, respectively. $|\mu_\xi|$, which equals $|\mathfrak{y}| \cos [150° - (\mathfrak{y}, \mathfrak{r})]$, and $|\mu_\phi|$, which equals $|\mathfrak{y}| .\sin [150° - (\mathfrak{y}, \mathfrak{r})]$, are found to be 4.15D and 0.74D, respectively. The proton-dipole distance r, which equals $\sqrt{3}c$, is 5.80A. Since τ_w/c^3 equals 6.78, ζ_0 may be found graphically from Eq. (7) to be equal to 0.90. From ζ_0 are obtained values of g_1, g_2, h_1, and h_2 in Table II which when used in Eqs. (6a) and (6b) with the given values of D_i and D yield the magnitudes 7.3 and 15.1 for D_ξ and D_ϕ, respectively. From Eq. (6) is then obtained the value 0.70 for log $K_{A_xB_0}$.

The evaluation of log $K_{A_xB_0}$ for a parasubstituted benzenoid acid and that of log $[K_1/(K_2\sigma)]$ for a benzenoid polybasic acid follow similar lines. It is possible to reverse all these calculations to obtain the value of any one of the parameters discussed in this section from given values of the other parameters and the appropriate data for dissociation constants.

TABLE III. Structural parameters[a] for the metasubstituted benzoic acids, $m-XC_6H_4COOH$ in water at 25°C.

x	log $K_{A_xB_0}$ (Exp.)	τ_w A³	$(\mu, \mathfrak{r})$ °	c A	c_{Ext} A	c_{Rot} A	log $K_{A_xB_0}$ (Calc.)
NO_2	0.71[b]	255	140	3.35			0.70
CN	0.52[c]	265	140	3.55			0.52
F	0.34[b]	250	138	3.20	3.25	2.85	0.33
Cl	0.38[d]	255	139	3.20	3.35	2.95	0.37
Br	0.39[b]	260	140	3.20	3.40	3.00	0.37
I	0.35[b]	265	140	3.20	3.45	3.00	0.34
CH_3	−0.07[b]	255	40	3.30			−0.07
$C(CH_3)_3$	−0.10[e]	265	40	3.40			−0.10

[a] In the table, the values of τ_w are given to the nearest 5A³, those of $(\mu, \mathfrak{r})$ to the nearest degree, and those of c, c_{Ext}, and c_{Rot} to the nearest 0.05A.
[b] J. F. J. Dippy, Chem. Rev. **25**, 151 (1939).
[c] M. Kilpatrick and R. D. Eanes, J. Am. Chem. Soc. **65**, 589 (1943).
[d] B. Saxton and H. F. Meier, J. Am. Chem. Soc. **56**, 1918 (1934).
[e] J. B. Shoesmith and A. Mackie, J. Chem. Soc., p. 300 (1936).

PART III. APPLICATIONS OF THEORY TO THE SUBSTITUTED BENZOIC ACIDS

In this section the term "structural parameters" will refer to the cavity volume τ, or to its estimate, the van der Waals volume τ_w, the focal radius c, and the angle $(\mathfrak{y}, \mathfrak{r})$ which characterize the molecules in an acid-base equilibrium, while the term "electrical parameters" will refer to the magnitude of the substituent dipole moment $|\mathfrak{y}|$, the internal dielectric constant D_i of the molecules, and the solvent dielectric constant D.

By means of the electrostatic theory, the experimentally determined values of log $K_{A_xB_0}$ for the metasubstituted benzoic acids in water at 25°C together with the appropriate values of the electrical parameters and all the structural parameters except the focal radii c have been employed to calculate the magnitudes of c for these acids. The values of c thus computed are given in Table III. The values employed for τ_w, $(\mathfrak{y}, \mathfrak{r})$, and log $K_{A_xB_0}$(Exp.) the experimentally determined log $K_{A_xB_0}$ are also presented in Table III. The values of c_{Ext} and c_{Rot} in the table were computed in the manner outlined in Part II. The quantities log $K_{A_xB_0}$(Calc.), also tabulated, are the magnitudes of log $K_{A_xB_0}$ computed from the values of c, τ_w, and $(\mathfrak{y}, \mathfrak{r})$ in the table.

Inspection of Table III shows that c for the halogen substituted acids takes on values lying between c_{Ext} and c_{Rot}, respectively the upper limit and free-rotation estimates of the focal radius c computed from electron diffraction data. It is further to be noted that the values of c for the halogens are less than those for the other substituent groups while c for the methyl group is less than that for the tertiary butyl group. This observation is consistent with the fact that the polyatomic substituent groups possess bond

[19] J. W. Baker and L. G. Groves, J. Chem. Soc., p. 1147 (1939).
[20] G. Åkerlof, J. Am. Chem. Soc. **54**, 4125 (1932).
[21] L. A. Wooten and L. P. Hammett, J. Am. Chem. Soc. **57**, 2289 (1935).
[22] G. Åkerlof and O. A. Short, J. Am. Chem. Soc. **58**, 1241 (1936).

dipoles which are not attached directly to the aromatic nucleus[16, 23] so that the point dipoles characterizing these groups should be farther away from the benzene ring than those of the halogens.

TABLE IV. $\log K_{A_xB_0}$(Calc.)/$\log K_{A_xB_0}$(Exp.) for the metasubstituted benzoic acids, $m-XC_6H_4COOH$ in various solvents at 25°C.

Solvent	X = NO_2	F	Cl	Br	I	CH_3
Glycol	0.83	0.84	0.75	0.74	0.73	0.9
Methanol	0.76	0.71	0.66	0.67	0.67	0.9
Ethanol	0.72	0.72	0.67	0.66	0.63	0.9
n-Propanol	0.76	0.75	0.72	0.71	0.65	0.8
n-Butanol	0.83	0.98	0.78	0.79	0.72	0.8
Dioxane-water, 26.5 wt. %	0.82	0.83	0.86	0.88	0.95	0.6
Dioxane-water, 43.5 wt. %	0.78	0.85	0.81	0.83	0.90	0.5
Dioxane-water, 61.0 wt. %			0.84			
Dioxane-water, 73.5 wt. %	0.90	0.88	0.87	0.90	0.93	0.6
Hypothetical, by extrapolation to $D=\infty$.	1.22	1.08	1.10	1.07	1.17	0.9

The reasonableness of the magnitudes and of the order of the values of the focal radii c of the metasubstituted benzoic acids constitutes good evidence that the electrostatic theory, assuming oblate spheroidal molecules, satisfactorily accounts for the relative acid strengths of these compounds.

The differences in Table III between $\log K_{A_xB_0}$(Exp.) and $\log K_{A_xB_0}$(Calc.) represent unavoidable errors introduced into the computations by rounding-off the values of c and by uncertainties in making and reading the large scale graphs used in the calculations. It is to be noted, however, that the set of structural parameters in the table is not the only possible one. On the average, increases in c of 0.1A, in τ_w of 25A^3, and in D_i of 1 unit cause a decrease in $\log K_{A_xB_0}$ of between fifteen and twenty percent, an increase of between twelve and fifteen percent, and a decrease of thirty percent, respectively. Variations in c and τ of the magnitudes given and in D_i of one-half unit, occurring in such directions as to leave $\log K_{A_xB_0}$(Calc.) unchanged, would yield values of these parameters as reasonable as those in Table III. However, for the sake of consistency, the conventions described in Part II for determining these parameters have been retained.

Values of $\log K_{A_xB_0}$ for the metasubstituted benzoic acids in solvents other than water have been calculated by the use of the same structural and electrical parameters employed to compute $\log K_{A_xB_0}$(Calc.) in water with the exception that the dielectric constant of each solvent considered has been substituted for that of water. The ratios of these calculated values to the experimental ones of Elliott[2] in *n*-propanol and of Elliott and Kilpatrick[1] for all the other solvents are given in Table IV. As has been pointed out by Elliott and Kilpatrick[1] in connection with the work of Westheimer and Kirkwood[10] and as is further indicated by the results in Table IV, the values of $\log K_{A_xB_0}$ calculated by the cavity model theory with the structural parameters successfully used for water solution are lower than the observed values in all actual solvents other than water.

An explanation of this lack of agreement between calculated and experimental values of $\log K_{A_xB_0}$ shown in Table IV may be found in the probability that the cavity volumes τ of acid and base solute molecules in solvents other than water are greater than those in water. Since the solvents other than pure water are made up of molecules which are larger than those of water itself, it would be expected that the interstitial spaces, and consequently the cavity volumes τ, in these solvents should be greater than those in water. The extent of the increase in τ required to bring about agreement between the calculated and experimental values of $\log K_{A_xB_0}$ in solvents other than water may be inferred from the data in Table V. The values of τ in this table have been calculated from the experimental values of $\log K_{A_xB_0}$, the appropriate electrical parameters and the structural parameters c and (μ, τ) of Table III.

TABLE V. Values of τ in A^3 for metasubstituted benzoic acids, $m-XC_6H_4COOH$ in various solvents.

Solvent	X = NO_2	F	Cl	Br	I	CH_3
Water	255	250	255	260	265	255
Glycol	305	325	340	360	370	295
Methanol	340	380	410	420	425	335
Ethanol	370	375	405	425	450	295
n-Propanol	350	360	395	410	460	335
n-Butanol	320	360	360	360	410	335
Dioxane-water, 26.5 wt. %	300	305	300	290	285	450
Dioxane-water, 43.5 wt. %	320	300	320	315	300	535
Dioxane-water, 61.0 wt. %			315			
Dioxane-water, 73.5 wt. %	295	310	300	300	290	535
Hypothetical, by extrapolation to $D=\infty$.	215	235	225	240	225	285

As would be expected, inspection of Table V reveals that, for each acid, τ increases continuously in magnitude in the series of solvents beginning with water and ending with *n*-propanol, the difference in τ for ethanol and *n*-propanol not

[23] L. E. Sutton, Proc. Roy. Soc. **A133**, 668 (1931).

TABLE VI. $\Delta \log K_{A_xB_0}$ for parasubstituted acids $p-XC_6H_4COOH$ in various solvents at 25°C.

Solvent	X = NO_2	CN	F	Cl	Br	I	CH_3	$C(CH_3)_3$
Water	0.30	0.30	−0.17	−0.03	−0.03		−0.12	−0.12
Glycol	0.25		−0.18	−0.09	−0.03	0.00	−0.10	
Methanol	0.24		−0.22	−0.11	−0.05	−0.02	−0.11	
Ethanol	0.29		−0.17	−0.05	−0.01	0.01	−0.11	
n-Propanol	0.28		−0.19	−0.08	−0.05	−0.01	−0.13	
n-Butanol	0.29		−0.11	−0.07	−0.04	−0.04	−0.11	
Dioxane-water, 26.5 wt. %	0.34		−0.15				−0.14	
Dioxane-water, 43.5 wt. %	0.40		−0.09	0.01	0.03	0.08	−0.11	
Dioxane-water, 61.0 wt. %				0.02				
Dioxane-water, 73.5 wt. %	0.35		−0.15	−0.03	0.02	0.02	−0.09	
Pure solvent average	0.28		−0.17	−0.07	−0.04	−0.01	−0.11	
Mean deviation	0.02		0.02	0.02	0.02	0.02	0.01	
Mixed solvent average	0.36		−0.13	0.00	0.02	0.05	−0.11	
Mean deviation	0.02		0.03	0.02	0.02	0.03	0.02	

being significant. (The erratic behavior of τ for *m*-toluic acid arises from the large relative error in the experimental values of $\log K_{A_xB_0}$ for this acid.) The decrease in τ exhibited by each acid on going down the series from the solvent *n*-propanol to the solvent *n*-butanol cannot at present be explained. The cavity volume calculated for each acid in the dioxane-water mixtures does not vary greatly with the concentration of dioxane. Unmixing of the solvent giving rise to a relatively constant environment around the acid and base molecules may serve to explain this fact.[24, 25] The free energy increment, due to this unmixing, which contributes to the value of $\log K_{A_xB_0}$ cannot at present be taken into account.[25] In subsequent computations cognizance is taken of the change of τ for an acid from solvent to solvent.

The structural parameters of Tables III and V together with the values of the electrical parameters discussed in Part II have been employed to compute $\log K_{A_xB_0}$ for the parasubstituted benzoic acids. The values thus obtained have been subtracted from the corresponding experimental values[1, 2] to yield the quantities $\Delta \log K_{A_xB_0}$ given in Table VI. The two averages of this quantity for each acid taken over the set of pure and mixed solvents, respectively, together with their mean deviations, are also shown in the table.

The values of $\Delta \log K_{A_xB_0}$ in Table VI for each parasubstituted acid are practically constant from one pure solvent to another. In dioxane-water mixtures the results in the table indicate that $\Delta \log K_{A_xB_0}$ for each acid is algebraically greater than in the pure solvents, although there are insufficient data to make certain of the constancy of that quantity with change of concentration of dioxane. This difference between one-component and mixed solvents may be connected with the possibility of variations in the free energy of unmixing[24, 25] of the mixed solvent by the molecules present in it on going from meta compounds to their para isomers.

It is desirable at this point to compare the results for $\log K_{A_xB_0}$ of parasubstituted benzoic acids obtained by means of the prolate spheroidal model of Westheimer and Kirkwood[10, 26] with those obtained by the author employing the oblate spheroidal model. The assumptions made in the comparison are that the molecule of a parasubstituted benzoic acid is to be represented by either a prolate spheroidal or an oblate spheroidal cavity of a given volume τ and that the length of the focal line of the prolate spheroid equals that of the focal diameter of the oblate spheroid so that the interprotonic distance for each model is the same. On this basis it is found that the absolute magnitudes of $\log K_{A_xB_0}$ as given by the prolate spheroidal model are from zero to fifteen percent greater than those yielded by the oblate spheroidal model. In explanation of this difference it may be shown that the foci of the prolate spheroidal cavity are farther distant from the boundary surface than is the focal circle

[24] J. L. Magee, T. Ri, and H. Eyring, J. Chem. Phys. 9, 419 (1941).
[25] G. Scatchard, J. Chem. Phys. 9, 34 (1941).
[26] Tables of values of functions required for the calculations were kindly supplied by F. H. Westheimer in a private communication to M. Kilpatrick.

in the oblate spheroidal cavity. Thus the effective dielectric constant for the interaction of the substituent dipole with the dissociating proton is nearer the internal molecular constant and therefore lower for the prolate spheroidal cavity model than for the oblate spheroidal model. Accordingly, $|\log K_{A_xB_0}|$ as calculated by the former model would be greater than that computed by the use of the latter.

On the basis of the constancy of $\Delta \log K_{A_xB_0}$ with change of pure solvent, it is possible to use the values of $\log K_{A_xB_0}$ of the meta and para isomers of a substituted benzoic acid with a symmetrical substituent in one pure solvent and the values of $\log K_{A_xB_0}$ for one of the isomers in a number of other solvents to predict $\log K_{A_xB_0}$ of the other isomer in the latter solvents.

During the course of the measurements by Kilpatrick and Eanes[27] of $\log K_{A_xB_0}$ for the cyanobenzoic acids at 25°C, the author predicted the values of $\log K_{A_xB_0}$ for the meta isomer in glycol, methanol, and ethanol from the already determined data for the meta isomer in water and for the para isomer in all four solvents. The structural parameters for the cyanobenzoic acids in water solution determined from $\log K_{A_xB_0}$ for the meta isomer in water are recorded in Table III. From these parameters and the experimentally determined value of $\log K_{A_xB_0}$, for the para isomer in water was calculated the value of $\Delta \log K_{A_xB_0}$ 0.30, given in Table VI, for para-cyanobenzoic acid. This value of $\Delta \log K_{A_xB_0}$, assumed constant in all the alcohols, was subtracted from the experimental values of $\log K_{A_xB_0}$ for the para acid in these solvents to yield new values of $\log K_{A_xB_0}$ consistent with the electrostatic theory developed by the author. From these last results, the values of c and $(\mu, \mathbf{r})$ in Table III, and the appropriate electrical parameters, values of D_f and thence of ζ_0 were determined for the cyanobenzoic acids in each solvent. These values of ζ_0 permitted the determination of D_f and D_ϕ for the meta acid in each alcoholic solvent. These last values of D_f and D_ϕ together with the values of c and $(\mu, \mathbf{r})$ in Table III and the value of $|\mu|$ given in Part II yielded the desired values of $\log K_{A_xB_0}$ which are given in Table VII in the column marked $\log K_{A_xB_0}$(Calc.).

[27] M. Kilpatrick and R. D. Eanes, J. Am. Chem. Soc. 65, 589 (1943).

The agreement between theory and experiment is considered to be good.

The quantity $\Delta \log K_{A_xB_0}$ for a substituted benzoic acid in a one-component solvent at a given temperature may be regarded as providing a numerical measure of the effect on the acid strength of the acid group due to the resonance interaction[13] of the substituent group in the para position with the benzene ring, the acid group, and its conjugate base group. The values of $\Delta \log K_{A_xB_0}$ in Table VI indicate that the acid-strengthening effect of the nitro and cyano groups is practically the same. There is also clearly exhibited the well-recognized[28] decrease of the acid-weakening effect due to resonance interactions of parasubstituted halogens in the order F > Cl > Br > I. The almost equal values of $\Delta \log K_{A_xB_0}$ for the methyl and tertiary butyl groups are to be noted. It would be expected that the absolute magnitude of $\Delta \log K_{A_xB_0}$ for the tertiary butyl group would be less than that for the methyl group since it is thought[29, 30] that the latter group can conjugate with the benzene ring more readily than the former. This point of disagreement would bear experimental investigation and verification.

TABLE VII. $\log K_{A_xB_0}$ for cyanobenzoic acids.

Solvent	$\log K_{A_xB_0}$ (Exp.) Para acid	$\log K_{A_xB_0}$ (Exp.) Meta acid	$\log K_{A_xB_0}$ (Calc.) Meta acid
Water	0.65	0.52	
Glycol	0.82	0.72	0.73
Methanol	0.91	0.83	0.82
Ethanol	1.00	0.97	0.94

The invariance of $\Delta \log K_{A_xB_0}$ with change of solvent can be made to appear quite reasonable on the following basis. It may be presumed[13, 16] that the extra acid-strengthening or acid-weakening effect of a para substituent arises from the difference in contributions of the paraquinoidal structures (more important than the orthoquinoidal structures) to the final fused structures of the para acid and its conjugate base, and the consequent difference in resonance stabilization.

[28] H. B. Watson, *Modern Theories of Organic Chemistry* (Clarendon Press, Oxford, 1941), second edition.

[29] J. W. Baker and W. S. Nathan, J. Chem. Soc., p. 1844 (1935).

[30] R. S. Mulliken, C. A. Ricke, and W. G. Brown, J. Am. Chem. Soc. **63**, 41 (1941).

The paraquinoidal resonance should tend to locate an accumulation of charge on the ring carbon atom adjacent to the acid group. The potential energy and, therefore, the relative contribution of the paraquinoidal form to the resonance should then be largely governed by the electrostatic interaction of the acid group dipole or the conjugate base group charge, as the case may be, with the adjacent accumulated charge. This interaction should occur relatively deep within the molecule across a short distance. The solvent dielectric constant should, therefore, contribute little to the effective dielectric constant for the interaction. Accordingly, the relative contributions of the paraquinoidal forms to the resonance should be little affected by change of solvent and the value of $\Delta \log K_{A_xB_0}$ should not change much.

In connection with the constancy of $\Delta \log K_{A_xB_0}$ it is recognized that all the solvents considered in this work have been hydroxylic solvents. Thus there have not occurred any great changes in the type of solvation of the molecules considered. It is probable that change of solvent type might introduce complications.

The author has attempted calculations, similar to those for the substituted benzoic acids, for the substituted phenols, thiophenols, anilinium ions, *N*, *N*-dimethylanilinium ions, and phenylboric acids. Some interesting results have been obtained, but the lack of large quantities of consistent experimental data, such as those available for the benzoic acids, introduces considerable ambiguity into the fixing of structural parameters. Accordingly, the whole treatment of these acids by means of the theory has been rendered very uncertain.

For the benzenoid polycarboxylic acids, the situation with respect to the scarcity of consistent experimental data is much the same as for the acids mentioned in the last paragraph. On application to the existing data the electrostatic theory of the author seems to give no more satisfactory results than do those of Bjerrum[3] and of Kirkwood and Westheimer.[9,10,12] The accumulation of more experimental data on the acidity of the substituted benzenoid acids, other than the benzoic acids, and the benzenoid polybasic acids is highly desirable.

PART IV. DERIVATION OF THEORETICAL RESULTS

The results presented in Part I are now to be derived. The electrostatic potential V in charge-free space within and without the oblate spheroidal surface ζ_0, separating a molecule of dielectric constant D_i from a continuous solvent medium of dielectric constant D, must satisfy Laplace's equation,[14]

$$\frac{\partial}{\partial\zeta}\left[(1+\zeta^2)\frac{\partial V}{\partial\zeta}\right]+\frac{\partial}{\partial\eta}\left[(1-\eta^2)\frac{\partial V}{\partial\eta}\right]+\frac{\zeta^2+\eta^2}{(1+\zeta^2)(1-\eta^2)}\frac{\partial^2 V}{\partial\phi^2}=0 \quad (8)$$

in the oblate spheroidal coordinates of Eq. (1). The potential inside ζ_0 due to the charges $e_1, e_2, \cdots, e_\nu$ characterizing the charge distribution of the molecule may be written[10,31] in the form,

$$V_i=\sum_{k=1}^{\nu}\frac{e_k}{D_i|\varrho-\varrho_k|}+\sum_{n=0}^{\infty}\sum_{m=-n}^{n}A_n{}^m P_n{}^{|m|}(i\zeta)T_n{}^{|m|}(\eta)\exp(im\phi), \quad (9)$$

where the $A_n{}^m$ are constants, ϱ and ϱ_k are radius vectors from a point, fixed with respect to the molecule, to the field point (ζ, η, ϕ) and to the charge e_k, respectively, and the $T_n{}^{|m|}(\eta)$ and $P_n{}^{|m|}(i\zeta)$ are the associated Legendre functions of the first kind defined respectively for real independent variable with absolute magnitude less than unity, and for imaginary independent variable.[14] The first term on the right of Eq. (9) may be expanded[14,31] in the form,

$$\sum_{k=1}^{\nu}\frac{e_k}{D_i|\varrho-\varrho_k|}=\sum_{n=0}^{\infty}\sum_{m=-n}^{n}\frac{E_n{}^m}{D_i}Q_n{}^{|m|}(i\zeta)T_n{}^{|m|}(\eta)\exp(im\phi), \quad (10)$$

where

$$E_n{}^m=\frac{i}{c}(2n+1)\left\{\frac{(n-|m|)!}{(n+|m|)!}\right\}^2(-1)^{|m|}\times\sum_{k=1}^{\nu}e_k P_n{}^{|m|}(i\zeta_k)T_n{}^{|m|}(\eta_k)\exp(-im\phi_k),$$

[31] T. M. MacRobert, *Spherical Harmonics* (Methuen and Company, Ltd., London, 1927).

where the $Q_n^{|m|}(i\zeta_k)$ are the associated Legendre functions of the second kind defined for imaginary independent variable.[14] The charges e_k of Eq. (10) are assumed to be located at the points $(0, \eta_k, \phi_k)$. In order to fulfill the condition that it vanish at an infinite distance from the charges e_k, the potential V_e outside the ellipsoid ζ_0 must take the form,[31]

$$V_e=\sum_{n=0}^{\infty}\sum_{m=-n}^{n}B_n^m Q_n^{|m|}(i\zeta)T_n^{|m|}(\eta) \times\exp(im\phi). \quad (11)$$

The quantities V_i and V_e must satisfy the boundary conditions[14] that the potential and normal component of electric displacement be continuous at all points on the spheroid ζ_0, which may be written in the form,

$$V_i(\zeta_0, \eta, \phi)=V_e(\zeta_0, \eta, \phi), \quad -1\leq\eta\leq 1, \quad 0\leq\phi\leq 2\pi \quad (12)$$

and

$$D_i\left(\frac{\partial V_i(\zeta, \eta, \phi)}{\partial\zeta}\right)_{\zeta=\zeta_0}=D\left(\frac{\partial V_e(\zeta, \eta, \phi)}{\partial\zeta}\right)_{\zeta=\zeta_0}.$$

Equations (9) and (11) are substituted into Eq. (12) and advantage taken of the orthogonality of the functions $T_n^{|m|}(\eta)$ over the range, $-1\leq\eta\leq 1$, and $\exp(im\phi)$ over the range, $0\leq\phi\leq 2\pi$, to yield a set of linear relations between the constants A_n^m and B_n^m, which by a simple rearrangement become

$$\frac{E_n^m}{D_i}Q_n^{|m|}(i\zeta_0)+A_n^m P_n^{|m|}(i\zeta_0)=B_n^m Q_n^{|m|}(i\zeta_0), \quad (13)$$

and

$$E_n^m Q_n'^{|m|}(i\zeta_0)+A_n^m D_i P_n'^{|m|}(i\zeta_0)=B_n^m D Q_n'^{|m|}(i\zeta_0),$$

where the quantities $P_n'^{|m|}(i\zeta_0)$ and $Q_n'^{|m|}(i\zeta_0)$ are the derivatives of $P_n^{|m|}(i\zeta)$ and $Q_n^{|m|}(i\zeta)$ evaluated at $\zeta=\zeta_0$. The solutions of Eqs. (13) for the quantities A_n^m are

$$A_n^m=E_n^m\left[\frac{1}{D}-\frac{1}{D_i}\right] \times\frac{Q_n^{|m|}(i\zeta_0)Q_n'^{|m|}(i\zeta_0)}{P_n^{|m|}(i\zeta_0)Q_n'^{|m|}(i\zeta_0)-(D_i/D)Q_n^{|m|}(i\zeta_0)P_n'^{|m|}(i\zeta_0)}. \quad (14)$$

The recurrence formula,[14]

$$i\Theta_n'^{|m|}(i\zeta)=\frac{|m|\zeta\Theta_n^{|m|}(i\zeta)}{1+\zeta^2}+\frac{\Theta_n^{|m|+1}(i\zeta)}{(1+\zeta^2)^{\frac{1}{2}}}, \quad (15)$$

where $\Theta_n^m(i\zeta)$ may be replaced by either $P_n^m(i\zeta)$ or $Q_n^m(i\zeta)$, may be used to transform Eq. (14) into the relation,

$$A_n^m=E_n^m\left[\frac{1}{D}-\frac{1}{D_i}\right] \times\frac{Q_n^{|m|}(i\zeta_0)}{P_n^{|m|}(i\zeta_0)}\left[1-\frac{D_i}{D}Y_n^{|m|}\right]^{-1}, \quad (16)$$

where

$$Y_n^{|m|}=\frac{|m|\zeta_0+(1+\zeta_0^2)^{\frac{1}{2}}P_n^{|m|+1}(i\zeta_0)/P_n^{|m|}(i\zeta_0)}{|m|\zeta_0+(1+\zeta_0^2)^{\frac{1}{2}}Q_n^{|m|+1}(i\zeta_0)/Q_n^{|m|}(i\zeta_0)}.$$

The work W required to form the molecule by bringing the charges $e_1, \cdots, e_r$ from initial positions of infinite separation in the solvent may be computed by substituting Eqs. (9) and (16) in the relation,

$$W=\tfrac{1}{2}\sum_{l=1}^{r}e_l\psi(0, \eta_l, \phi_l), \quad (17)$$

where $\psi(0, \eta_l, \phi_l)$ is the potential V_i at the location of the charge e_l, assuming e_l to have been removed after all the other charges present are fixed in place.

It is now possible to evaluate the quantity ΔW of Eq. (2) for the equilibrium between the molecules A_1, B_2, A_2, and B_1, where all the molecules are bounded by oblate spheroids ζ_0 and possess identical charge configurations except for the fact that A_1 and B_1 have similarly placed charges $e_1, \cdots, e_s$ in excess over the molecules A_2 and B_2, respectively. On the basis of these assumptions the use of Eqs. (9), (16), (17), and (2), followed by replacement of the quantities $P_n^{|m|}(i\cdot 0)$ and $T_n^{|m|}(0)$ by their values in terms of n and m, yields the relation,

$$\Delta W=e\sum_{k=1}^{s}\frac{e_k}{D_i r_k} +\frac{i}{c}\left[\frac{1}{D}-\frac{1}{D_i}\right]\sum_{\substack{n=0\\(n+m)\text{ even}}}^{\infty}\sum_{m=-n}^{n}L_n^m(-1)^{(3n+|m|)/2}$$

$$\times\frac{(2n+1)[(n-|m|)!]^2(n+|m|)!}{\left\{2^n\left(\frac{n-|m|}{2}\right)!\left(\frac{n+|m|}{2}\right)!\right\}^3}$$

$$\times\frac{Q_n^{|m|}(i\zeta_0)}{P_n^{|m|}(i\zeta_0)}\left[1-\frac{D_i}{D}Y_n^{|m|}\right]^{-1}, \quad (18)$$

where

$$L_n^m=e\sum_{k=1}^{s}e_kT_n^{|m|}(\eta_k)\exp(-im\phi_k).$$

The symbol e represents a dissociating proton located at the point (0, 0, 0) and r_k the distance of the kth among the charges $e_1, \cdots, e_s$ from the proton e. In the case of the symmetrical dibasic acids the charges $e_1, \cdots, e_s$ reduce to the single proton e placed on the focal circle at the point (0, 0, Φ), and r_k in Eq. (18) becomes the single quantity r, the interprotonic distance, while L_n^m may be rewritten in the form,

$$L_n^m=e^2\frac{(-1)^{(n-|m|)/2}(n+|m|)!}{2^n\left(\frac{n-|m|}{2}\right)!\left(\frac{n+|m|}{2}\right)!}$$

$$\times\exp(-im\Phi). \quad (19)$$

Replacement of the first summation in Eq. (18) by the term $e/(D_ir)$ and use of Eq. (19) yield an expression for ΔW which, after application of Euler's formula for the cosine, may be combined with the form of Eq. (2) applicable to dibasic acids to yield Eq. (3).

When substituent effects are being considered, the charges $e_1, \cdots, e_s$ are replaced by a positive charge q at $(0, \eta, \Phi+\Delta\phi)$ and a negative charge $-q$ at (0, 0, Φ). The line vector from $-q$ to q is written $\boldsymbol{\Delta s}$. It is then assumed that the positive charge approaches the negative charge, and, at the same time, the absolute magnitude q of each increases in such a way that

$$\lim_{\substack{\Delta s\to 0\\ q\to\infty}} q\boldsymbol{\Delta s}=\boldsymbol{\mu}, \quad (20)$$

where $\boldsymbol{\mu}$ is a point dipole, representing the substituent dipole, at (0, 0, Φ). The dipole $\boldsymbol{\mu}$ has components along the unit vector $\mathbf{i}_1$ directed from the center of the focal circle through the point (0, 0, Φ) and along the unit vector $\mathbf{i}_2$ tangent to the focal circle in the direction of increasing ϕ. On this basis, in Eq. (18),

$$e\sum_{k=1}^{s}\frac{e_k}{D_ir_k}\to-\frac{e\boldsymbol{\mu}\mathbf{r}}{D_ir^3}, \quad (21)$$

where $\mathbf{r}$ is the line vector from the dissociating proton to the dipole $\boldsymbol{\mu}$ and r is its absolute magnitude, while

$$L_n^m=e\boldsymbol{\mu}\Big[\mathbf{i}_1\exp(-im\Phi)$$

$$\times\lim_{\eta\to 0}\frac{T_n^{|m|}(\eta)-T_n^{|m|}(0)}{c(1-\eta^2)^{\frac{1}{2}}-c}+\mathbf{i}_2T_n^{|m|}(0)$$

$$\times\lim_{\Delta\phi\to 0}\frac{\exp[-im(\Phi+\Delta\phi)]-\exp(-im\Phi)}{c\Delta\phi}\Big]$$

$$=\frac{(-1)^{(n-|m|)/2}(n+|m|)!}{2^n\left(\frac{n-|m|}{2}\right)!\left(\frac{n+|m|}{2}\right)!}$$

$$\times\exp(-im\Phi)\frac{e\boldsymbol{\mu}}{c}$$

$$\times[\mathbf{i}_1(n^2-|m|^2+n)-\mathbf{i}_2(-1)^{\frac{1}{2}}m]. \quad (22)$$

Substitution of Eqs. (21) and (22) in Eq. (18), followed by the use of Euler's formulas for the sine and cosine, yields a result which, when combined with the appropriate special case of Eq. (2), gives rise to Eq. (4). On account of symmetry, a component of the dipole in a direction perpendicular to the plane of the focal ring makes no contribution to ΔW.

The author wishes to thank Drs. Martin Kilpatrick and Enos E. Witmer for their helpful advice and unfailing interest in his work and Dr. J. A. Shohat for suggestions which greatly facilitated the calculations. He is also indebted to the University of Pennsylvania for granting him a Harrison Fellowship for the year 1936–37.

THE JOURNAL OF CHEMICAL PHYSICS VOLUME 12, NUMBER 7 JULY, 1944

The Thermodynamic Properties and Potential Energy of Solid Argon

O. K. RICE

University of North Carolina, Chapel Hill, North Carolina

(Received April 1, 1944)

In an earlier paper an attempt was made to obtain the interatomic potential for a pair of argon atoms, using the specific heat data at low temperatures and a theory in which the Debye characteristic temperature Θ was related to the curvature of the interatomic potential energy curve. Difficulties in accounting for certain other experimental data were explained on the supposition that disorder sets in in the solid below the melting point. As there are certain objections to this point of view, a new calculation is presented herewith in which the Debye theory is assumed to hold throughout, and Θ and the potential energy of the solid are calculated independently of each other from the available experimental data on the specific heat at low temperatures, and on the equation of state at high pressures. A consistent picture of the thermodynamic properties of solid argon is thus obtained, but the interatomic potential curve for a pair of atoms differs greatly from that obtained by the method used previously. The interatomic potential curve found here shows extreme change in curvature near the minimum. This change in curvature is so great that, if the result is correct, the theory of small vibrations will not be applicable, and it will not be possible to relate Θ to the curvature, as was done in the earlier work. The significance of this conclusion for the theory of the solid state is discussed.

1. INTRODUCTION

RECENTLY I made an attempt to find the interatomic potential energy curve for argon by means of a detailed consideration of the properties of the solid, assuming additivity of the potential energy of different pairs of atoms, and using the theory of small vibrations.[1] It was possible to correlate many of the properties of the solid and to obtain a reasonable potential energy curve; however, a difficulty appeared, in that it was hard to understand the high value of the internal pressure $(\partial E/\partial V)_T$, derived from the work of Simon and Kippert.[2] Further difficulties appeared later when, in unpublished work, I attempted to extend this calculation to high temperatures and pressures. At 193°K it was found that the calculated pressure compatible with the molal volume of the solid in equilibrium with the liquid was about three times too low. In other words, the theoretical solid was much more compressible than the actual one. To explain the discrepancy with Simon and Kippert's work, I had already suggested the appearance of disorder* in the solid, even at a temperature considerably below the normal melting point. Such an appearance of disorder would also change the properties in the right direction to explain the difficulties around 193°K, but the extent of disorder required would be very great. If we suppose that the discrepancies between the observed and calculated energies in Table II of my previous article[1] are typical of what would be expected for the energy which would have to be ascribed to energy of disorder, it is seen that something like half an entropy unit of entropy of disorder would have to be introduced up to the melting point. It is certainly to be anticipated that considerably more than this would be introduced at 193°K, even though the solid under consideration at the higher temperature is somewhat more compressed. In fact, from this point of view it might be expected, though perhaps one could not be absolutely certain, that the difference between the solid and the liquid would be wiped out, and that there would be no sharp melting point. Actually a sharp melting point is observed, and there is every evidence that this will continue to be the case even at considerably higher temperatures.

On closer examination it may also be seen that the introduction of disorder to explain Simon and Kippert's value of $(\partial E/\partial V)_T$ for the solid at normal pressures leads to certain difficulties which are rather hard to explain away.

[1] O. K. Rice, J. Am. Chem. Soc. **63**, 3 (1941).
[2] F. Simon and F. Kippert, Zeits. f. physik. Chemie **135**, 113 (1928).
* By disorder we mean here actual irregularities in the lattice structure. See below, last paragraph of Section 1.

It is to be expected that the disorder in the solid would be setting in more and more rapidly as the melting point was approached. Since the effect is considerable, we should expect that $(\partial S/\partial V)_T$, or $(\partial P/\partial T)_V$ (its thermodynamic equivalent and the quantity actually measured by Simon and Kippert), which would otherwise vary but little, would almost certainly increase between 73°K and the melting point.

Actually they found $(\partial P/\partial T)_V$ at 73° to be 38 atmos./degree, while Clusius and Weigand[3] found the rate of increase of the pressure of the *melting* solid with the melting point to be 39 atmos./degree. Since the volume of the melting solid decreases with increasing temperature, $(\partial P/\partial T)_V$ at the melting point must be less than 39 atmos./degree, and so, insofar as the data of different investigators are comparable, the indications are that $(\partial P/\partial T)_V$ is probably *less* at the melting point than it is at 73°K. While the possibility of disorder in the solid cannot, perhaps, be definitely discarded on these grounds, this is certainly contrary to what intuition tells us to expect if disorder is playing an appreciable role in determining the properties of the solid.

These considerations make it seem desirable to reconsider the problem of solid argon, in order to see whether a consistent picture can be obtained on the assumption that the Debye theory applies throughout without modifications or complications. This is equivalent to saying that no disorder, in the sense I have used that word, occurs in the solid, since it is implied that all atoms are vibrating about points of equilibrium which form as undisturbed face-centered cubic lattice. On the other hand, I have decided to abandon the calculations which led in my earlier work to a relation between the potential energy, and the Debye characteristic temperature, Θ, of the solid, and determine these quantities independently by using all the available experimental data. The justification for this procedure will appear later.

2. THE THERMAL PROPERTIES OF ARGON AT LOW TEMPERATURES

If it is assumed that the Debye theory of the solid holds, it is possible, since the specific heat C_p has been measured up to the melting point[4], to calculate the entropy of solid argon at any temperature. The entropy depends only on the thermal motion of the atoms, and it can be expressed as a function of the ratio Θ/T of the characteristic temperature to the absolute temperature of the solid. This then enables us to obtain Θ as a function of the temperature. Θ, of course, is not constant, because of the expansion of the lattice with increasing temperature.

It is also possible, by integration under the C_p curve, to find the total energy E of the solid. Once Θ is known, the thermal energy E_t and the zero-point energy E_z can be obtained, whence the potential energy $E_p=E-E_t-E_z$ can be found. E_p is the energy which the crystal would possess if all the atoms were fixed at their equilibrium positions; the potential energy inherent in the vibratory motion is included in E_z and E_t.

It seems astonishing that the above-outlined program has not been carried out, in view of considerable work on the equation of state of argon,[5] practically all of which assumed the validity of Debye's theory; but I have not been able to find any such treatment, though both the necessary theoretical machinery and experimental data have been available for many years.

The results of the above-indicated calculations are shown in Table I. C_p for every odd degree from 11°K to 79°K, inclusive, was obtained by direct linear interpolation between the experimental values for the nearest temperatures, as given by Clusius; experimental errors were, thus, not smoothed off in the values obtained, half of which are given in Table I. Above 79°K and below 11°K, the values were obtained by extrapolation, the latter with the aid of the T^3 law. The value of E given is just $\int_0^T C_p dT$ obtained with good approximation by simple summation of the C_p values. S is $\int_0^T (C_p/T)dT$, obtained similarly. Θ/T (and hence Θ, which is tabulated) was obtained from S by the aid of the table given in Landolt-Börnstein.[6] E_z was di-

[3] K. Clusius and K. Weigand, Zeits. f. physik. Chemie **B46**, 1 (1940).

[4] K. Clusius, Zeits. f. physik. Chemie **B31**, 459 (1936).

[5] E.g., A. Eucken, Verh. d. Phys. Ges. **18**, 4 (1916); F. Simon and C. v. Simson, Zeits. f. Physik **25**, 160 (1924); K. F. Herzfeld and M. Goeppert-Mayer, Phys. Rev. **46**, 995 (1934); G. Kane, J. Chem. Phys. **7**, 603 (1939); O. K. Rice, reference 1.

[6] *1. Ergänzungsband* (1927), pp. 702–707. *Caution:* These tables contain occasional errors which, however, can usually be detected and corrected by noting successive differences.

rectly calculated from the formula, valid for the Debye solid

$$E_z = 9R\Theta/8, \quad (1)$$

where R is the gas constant. E_t and E_p were obtained as noted above, but in the case of E_p the zero of energy was changed to that of the gaseous state at 0°K, with the aid of the data on the specific heats of solid and liquid, the heat of fusion,[3] the heat of vaporization,[7a] and the heat of expansion of the gas.[7b] The heat of sublimation at 0°K was estimated to be 1851.5 cal. per mole, and taking the zero-point energy to be the same as at 24°K, the potential energy at 0°K was estimated to be −2035.1 cal. per mole. This may be in error by a few calories, which is not, however, of great importance as long as the *differences* in potential energy are correct to within a few tenths. The values of a (distance between nearest neighbors in the lattice) were calculated from Θ as indicated in the next section.

TABLE I. Properties of solid argon. Temperatures in °K; energy units, calories per mole; a in Angstrom units.

T	C_p*	E	S	Θ	E_z	E_t	$-E_p$	a
2	0.00	0.00	0.000					
4	0.02	0.04	0.014					
6	0.10	0.24	0.054	85.2		0.24		
8	0.29	0.82	0.136	83.4		0.81		
10	0.61	2.04	0.272	82.1		2.03		
12	1.06	4.16	0.464	81.1		4.11		
16	1.89	10.90	0.944	81.1		10.9		
20	2.64	20.76	1.492	81.6		20.9		
24	3.30	33.32	2.062	82.18	183.6	33.5	2035.3	3.8184
28	4.01	48.74	2.656	81.93	183.0	48.9	2034.7	3.8191
32	4.50	66.32	3.242	81.50	182.1	66.1	2033.4	3.8203
36	4.88	85.48	3.804	81.04	181.0	84.8	2031.9	3.8218
40	5.21	106.00	4.346	80.40	179.6	104.7	2029.8	3.8237
44	5.50	127.72	4.864	79.73	178.1	125.4	2027.3	3.8257
48	5.70	150.34	5.356	79.10	176.7	146.9	2024.7	3.8277
52	5.98	173.98	5.828	78.31	174.9	169.1	2021.5	3.8302
56	6.13	198.36	6.278	77.56	173.3	191.6	2018.0	3.8326
60	6.32	223.44	6.710	76.77	171.5	214.5	2014.1	3.8353
64	6.57	249.42	7.128	75.90	169.5	238.0	2009.6	3.8383
68	6.84	276.52	7.538	74.97	167.5	261.9	2004.3	3.8418
72	7.05	304.50	7.936	74.10	165.5	285.9	1998.4	3.8450
76	7.36	333.64	8.330	72.88	162.8	310.7	1991.4	3.8498
80	7.60	363.82	8.716	71.70	160.2	335.4	1983.2	3.8548
84	7.91	395.22	9.098	70.56	157.6	360.5	1974.4	3.8600

* C_p is not for the given T, but for $T-1°$.

We may note in passing that there is a rather anomalous behavior of Θ below 24°, similar to that found by Clusius when he calculated Θ from C_v, but less marked, because Θ is a more sensitive function of C_v than it is of S, which depends on the integral of the specific heat and, therefore, averages all values up to the temperature considered. Θ calculated from S is less sensitive to experimental error, but there is no advantage on this account in calculating it from S if deviations from the Debye theory are real. It is known from the work of Blackman and others that anomalies in the apparent value of Θ at extremely low temperatures may result from the fact that the frequency spectrum assumed by Debye is only an approximate one.[8] It is possible that some such effect is the cause of the behavior of Θ in the present case.[9] If this is true, while it affects the validity of the Debye theory at low temperatures, it in no way invalidates our considerations, which depend upon the data at higher temperatures.

3. DEDUCTIONS FROM EQUATION-OF-STATE DATA

In order to get Θ and E_p as functions of the primary variable V, the molal volume, or its equivalent a, the smallest interatomic distance in the lattice, use can be made either of the data of Simon and Kippert[2] on $(\partial P/\partial T)_V$, or those of Bridgman[10] on the equation of state at high pressures. Since Bridgman's data extended over a greater range of conditions, it was found that more detailed information could be obtained by proceeding from them.

Bridgman has measured the melting point, the molal volume of the melting liquid, and the ΔV of fusion over a range of pressures. From this it is possible to obtain the volume of the solid in equilibrium with the liquid, and its temperature, for pressures up to 6000 kg/cm². Under these conditions at 1, 2000, 4000, and 6000 kg/cm², respectively, Bridgman has given the following values of the volume of the solid: 0.622, 0.613, 0.610, and 0.607 cc/g. His value of ΔV at 1 kg/cm², however, is undoubtedly too small,[3] which means that his value for the volume of the solid is probably too large, and I have decided to replace the value 0.622 cc/g by the

[7] (a) A. Frank and K. Clusius, Zeits. f. physik. Chemie **B42**, 395 (1939). (b) Reference 1, Appendix II.

[8] See, e.g., F. Seitz, *Modern Theory of Solids* (McGraw-Hill Book Company, Inc., New York, 1940), Chapter III. However, the discussion of Section 4, below, indicates that the actual calculations, which are based on the theory of small vibrations, will not be applicable to a case like argon.

[9] My statement in reference 1 that this could not be true was based on the assumption that the deviation is in the wrong direction. This is not necessarily correct. It would be correct if the real frequency spectrum differed from the Debye spectrum only in containing a special band of high frequencies, but this is too restricted an assumption.

[10] P. W. Bridgman, Proc. Am. Acad. **70**, 1 (1935).

value 0.616 cc/g obtained by linear extrapolation. From these values of the volume, I have calculated the values of a, and have obtained a for 1000 kg/cm² by interpolation. The values of T, a, and P (changed to cal./cc) obtained from Bridgman's data (changed as indicated) are summarized[11] in the first three columns of Table II.

To relate these data with the function Θ we start with Grüneisen's equation for the pressure[12]

$$P=-(E_t/\Theta)d\Theta/dV-dE_z/dV-dE_p/dV, \quad (2)$$

which, from Eq. (1), may be recast into the form

$$P=-\Theta^{-1}(d\Theta/dV)(E_t+E_z)-dE_p/dV. \quad (3)$$

We may change to the variable a, and for a face-centered cubic lattice like argon, we obtain, if a is in angstroms and P in cal./cc,

$$P=-(1.278a^2)^{-1}\times[\Theta^{-1}(d\Theta/da)(E_t+E_z)-dE_p/da]. \quad (4)$$

Observing now that dE_p/da depends on a but not on the pressure, we may express it in terms of the equilibrium value of E_t+E_z for the given value of a and for $P=0$, obtaining thus

$$P=-(1.278a^2\Theta)^{-1}(d\Theta/da)\times[(E_t+E_z)-(E_t+E_z)_{P=0}]. \quad (5)$$

If Θ were known as a function of a, we could determine it for the cases presented in Table II, calculate from it E_t (for any desired temperature) and E_z; and, by interpolation in Table I, we could find $(E_t+E_z)_{P=0}$. Then by Eq. (5) we could calculate a value of P to compare with the observed values in Table II. The function for Θ which will reproduce these values of P will be unique over the range involved within the limits of error. It has been found that it is satisfactory to set

$$\Theta=70.56-211(a-3.86)+1650(a-3.86)^2. \quad (6)$$

This, when used as indicated above, gives the last column of Table II. Also, by comparison with the values of Θ in Table I, it gives the last column of Table I. Equation (6) is also consistent with the data of Simon and Kippert,[2] which are closely related to those of Bridgman. We note that in Eq. (4) the only quantity which depends on the temperature is E_t, if a is held constant, and we have $(\partial E_t/\partial T)_a=C_v$. Differentiating with respect to temperature, we have

$$(\partial P/\partial T)_V=-(1.278a^2\Theta)^{-1}(d\Theta/da)C_v. \quad (7)$$

Simon and Kippert, as stated above, have measured $(\partial P/\partial T)_V$ at 73°K and $P=0$, and have given as the value 38 atmos./deg. From Table I, we know the value of Θ, hence of Θ/T and C_v, under these conditions; from Eq. (6) we can obtain the value of a, and, by differentiating, $d\Theta/da$. We can thus calculate $(\partial P/\partial T)_V$ and find 43 atmos./deg., in very reasonable agreement with Simon and Kippert.

The equilibrium values of a for zero pressure, which have been calculated from Eq. (6) and included in Table I, are worthy of some remark. If they are correct, and it seems unlikely that they are far wrong, we may conclude that the volume expansion from 0°K to the melting point is of the order of 3 percent. This is considerably less than has been supposed to be the case. For example, in a recent article Fürth[13] has estimated the expansion to be about 7.5 percent. Simon and Kippert noting the high value of $d\Theta/dV$ obtainable from their results, and evidently having the idea that the total expansion of the solid must be even greater than 7.5 percent, made the statement that, between 0°K and the melting point, Θ should change by 70 percent. Of course, such a change in Θ appears highly improbable; the very fact that it was suggested indicates the great importance of having a reasonably close knowledge of the true thermal expansion.

From Table I it is possible to find E_p as a function of a. If we set $x=a-3.84$, it is found that the expression

$$-E_p=2006.8-1532x-5690x^2+205{,}000x^3-1{,}062{,}000x^4 \quad (8)$$

TABLE II. Equation of state at high pressures. Units as in Table I (P in cal./cm³).

T	a	P(obs.)	P(calc.)
106.4	3.85685	23.4	23.4
126.3	3.8537	46.9	46.5
161.9	3.8473	93.7	93.3
192.9	3.8411	140.6	141.7

[11] a is not known closer than to about 0.01A, but the differences in Table II may be significant to about 0.001A.

[12] For a simple derivation see Appendix I of reference 1.

[13] R. Fürth, Proc. Camb. Phil. Soc. **37**, 34 (1941).

gives a very good representation of the results. This is shown in Fig. 1, where the curve defined by Eq. (8) is compared with points taken directly from Table I. It may be of interest to note that the derivative of Eq. (8), and Eq. (6) and its derivative, together with the values of E_l+E_z from Table I, when set into the right-hand side of Eq. (4) make it equal to zero, as they should. This is, however, no proof of the theory. The values of all the quantities in Eq. (4) depend upon the assumption of the Debye theory, as does Eq. (4) itself. As far as the data we have available are concerned, Eq. (4) may be considered an identity. The beginnings of an experimental check of the fundamental assumption of the validity of the Debye theory could be obtained if the values of a could be determined experimentally at different temperatures. The agreement of the data of Simon and Kippert with the deductions from the data of Bridgman, does, however, offer some check on the consistency of the theory we have presented, over a wide range of pressures.

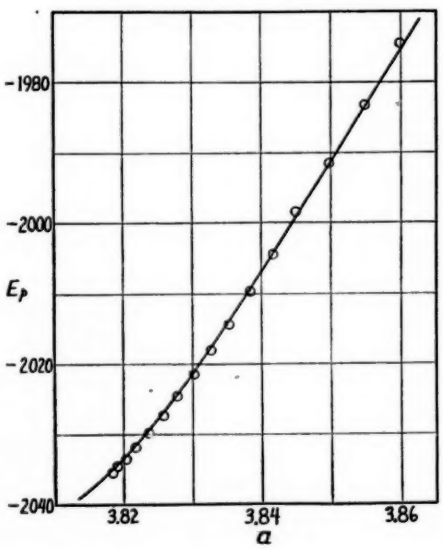

FIG. 1.

4. DISCUSSION OF THE THEORY OF THE SOLID STATE

Summarizing the deductions of the last two sections, our procedure has been to use the specific heat data, assuming the Debye theory, in order to find values of Θ and E_p for solid argon at various temperatures. These values of Θ and E_p were then correlated with the primary variable a by use of equation of state data, principally that at high pressures. In contrast to this procedure, in my earlier work on solid argon[1] no use, or at most, only incidental use, was made of the equation of state data, but, working through the interatomic potential-energy curve, and by means of a discussion of the equation of motion of an atom in the field of its neighbors, a relation was obtained between Θ and E_p. Using, then, the specific heat data, the correlation between Θ, E_p, and a was effected. The results obtained for E_p as a function of a turn out to be strikingly different in the two cases.

Actually, in my earlier article, the *interatomic* potential U for a single pair of atoms was given as a function of a. In order to get a comparison, an attempt may be made to find U from the values of E_p given in Table I, by assuming that the effect of atoms more distant than the nearest neighbors is correctly given by Buckingham's expression,[14] as assumed in the earlier paper. The result is shown as curve I in Fig. 2. The solid portion around the minimum comes from Eq. (8), and it is somewhat extrapolated beyond the range of the data. The broken portion of the curve is merely sketched in. For comparison is shown the curve previously derived,[1] assuming disorder to be present in the solid (curve II). The difference between the new curve and the old one, as well as all other previously derived curves, is very striking, the sharp bend at the minimum of curve I being especially noticeable. It appears that curve I can hardly reach the theoretical curve of Buckingham at the distance of the next nearest neighbors. This means a certain internal inconsistency in deriving curve I; a correction would raise the minimum somewhat, but would not be expected to change the shape appreciably. It seems probable that the data on the virial coefficient could now be used with some success to aid in fixing the actual curve.

The difference between curves I and II is far beyond any possibilities of error, once the procedure has been formulated even qualitatively. How, then, are these contradictory results to be

[14] R. A. Buckingham, Proc. Roy. Soc. London **A168**, 264 (1938).

explained? The difficulty seems to reside in the fact that my earlier calculations in common with all other calculations of this sort which have been made, assumed that the motion of an atom in the field of its neighbors could be handled by the method of small vibrations. If the new potential-energy curve obtained here is even roughly correct, this assumption must be completely erroneous. Even the amplitude of the zero-point vibration will be sufficient to cover a range of distances over which the curvature will vary enormously, may even change sign. The vibrations of individual atoms will, therefore, be anharmonic, and no relation between Θ and E_p based upon the ordinary theory of small vibrations can have any validity.

The question then arises, as to whether the Debye theory itself can retain any validity at all. The Debye theory is based upon a certain distribution of frequencies of normal vibrations. The process of setting up normal vibrations stems from the theory of small oscillations, and if any appreciable deviation from harmonicity occurs this process breaks down. It would thus seem that the Debye theory, and, therefore, also Grüneisen's equation, would break down with it. However, it does seem possible that one might superimpose an elastic wave, even one of short wave-length, on any atomic distribution, provided this elastic wave is itself of small amplitude. Actually, none of the individual normal vibrations of a solid will be of large amplitude; it is only the displacement of individual atoms, which is the resultant of the superposition of many such normal modes of vibration, which becomes of large amplitude. It seems, therefore, not unreasonable to suppose that the normal modes of vibration exist and are quantized in much the usual way, but that Θ is determined, not by the curvature of the force field in which an atom would find itself if all atoms were situated at their position of equilibrium, but rather by an average curvature of the fields of the atoms in their actual positions, which for the curve indicated in Fig. 1, would be considerably different. Since Θ might be expected to depend upon the average displacement of atoms from the position of equilibrium, it might be expected to be a function of the temperature even at constant volume. This, however, would

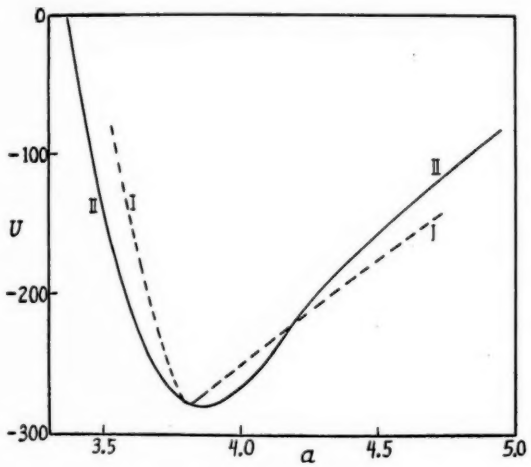

FIG. 2.

result in complications of a fundamental character, which could not be handled by the ordinary methods of statistical mechanics, and would certainly invalidate the Debye theory. In view of the considerable displacement which already exists at the absolute zero, on account of the zero-point energy, it may be that this variation in Θ with temperature is not so great but that we may assume that the assignment of a constant value of Θ for a system of fixed volume has an approximate significance.

Constancy of the Debye Θ with temperature depends upon the approximately even spacing, as in a harmonic oscillation, between the successive energy levels of the normal vibrations. It does not depend in any essential way on the exact level of the zero-point vibration. If, as seems probable, the rate of change of curvature is greatest near the minimum of the potential energy curve, it might well be expected that the relation of the zero-point energy to Θ would be affected, so that it would be no longer given by Eq. (1). If, however, E_z were still proportional to Θ, Eq. (3) would still hold, and the results would be altered only by a nearly (though not quite) constant change in E_z, and, consequently, a nearly constant increment to E_p, such as would not be expected to have a great effect on our fundamental conclusions.

The above discussion is admittedly highly speculative. Problems are involved here which would seem to require the opening of a new

chapter in the theory of the thermodynamic properties of solids. We use these remarks, however, as justification for the tentative assumption that even in this rather unfavorable case the Debye theory still offers a reasonable approximation, and that the values of Θ, E_p, and a, given in Table I, may be looked upon as not devoid of meaning in the same approximate sense.

THE JOURNAL OF CHEMICAL PHYSICS VOLUME 12, NUMBER 7 JULY, 1944

A Method for Determining Small Quantities of Oxygen

MANFRED POLLACK, PETER PRINGSHEIM, AND DOLORES TERWOORD*
Department of Chemistry, University of Chicago, Chicago, Illinois

(Received April 24, 1944)

A method is described which permits one to follow the production rate of minute quantities of oxygen. The method is based on the quenching of the phosphorescence of a dye adsorbed on silica gel. Examples of the application of the method are discussed.

THE possibility of determining the presence of minute quantities of oxygen by the quenching of the phosphorescence of a dye has been suggested by Kautsky.[1] The application of the method has been discussed in detail from the theoretical and experimental viewpoints by Franck and Pringsheim.[2] At present, the method is being employed successfully in this laboratory for measuring oxygen production as low as 5×10^{-8} cc at atmospheric pressure per minute.

If the problem consists only of ascertaining whether oxygen is evolved under given experimental conditions, it suffices to have the silica gel with its adsorbed phosphorescent dye in the same container as the material under observation, and to observe the intensity of the phosphorescence while the reaction occurs. This, however, would not enable one to follow a varying rate of oxygen production over a long time because the sensitivity of the method is high for only very low oxygen pressures; after a certain amount of oxygen has accumulated in the container an additional small quantity would not be detectable. It is necessary, therefore, to separate the phosphorescent gel (which, for the sake of brevity, will be called the phosphor) from the oxygen source and to transport the oxygen from the source through the phosphor by means of a steady stream of some inactive gas such as N_2. Because of the high sensitivity of the method the transporting gas must be of the highest purity. Therefore the apparatus consists of three main parts: the nitrogen purifying section, the oxygen source, and the phosphor with the phosphoroscope.

Tank nitrogen is passed through a vertical glass column containing finely divided copper adsorbed on Fuller's earth and heated to about 280°C. This technique, devised by Meyer and Ronge,[3] has the advantage that, because of the relatively low temperature needed for oxidation of the copper, the oxygen pressure corresponding to the presence of copper oxide is much lower than in the usual copper oven heated to 600°C. When a part of the column is discolored by oxidation it can be regenerated by passing H_2 through it for several minutes at the same temperature. Thus the same filling can be used indefinitely.

The further course of the gas stream is represented in Fig. 1. T_1 and T_2 are traps cooled with liquid nitrogen. B is a one-liter bulb closed by a manometer; this eliminates fluctuations in the gas flow and provides a means to control the overpressure necessary to overcome the flow resistance in the following parts of the apparatus.

* National Research Fellow, 1943–1944.

[1] H. Kautsky and A. Hirsch, Zeits. f. anorg. allgem. Chemie **222**, 126 (1935).

[2] J. Franck and P. Pringsheim, J. Chem. Phys. **11**, 21 (1943).

[3] F. B. Meyer and G. Ronge, Zeits. f. angew. Chemie **52**, 63 (1939).

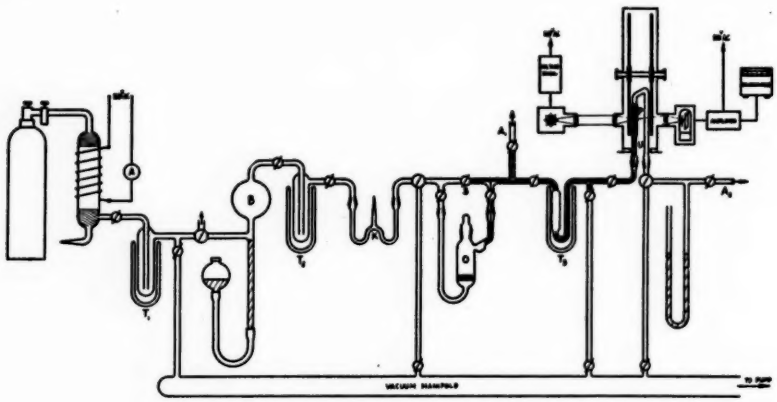

FIG. 1.

K is a tube into which a mirror of pure potassium is distilled. If the N_2 is sufficiently pure, the mirror retains its metallic reflecting surface; otherwise it rapidly becomes dull. It has been found necessary to have the whole system thoroughly evacuated up to the copper oven before filling with nitrogen; it is very difficult to remove the last traces of oxygen by simply flushing the line with pure N_2. The nitrogen treated in this manner can be admitted to the phosphor without any resultant quenching of the normal phosphorescence.

In our experiments, which were concerned with oxygen production by photosynthesis, the oxygen source O consisted of a suspension of plant matter (algae or macerated leaves) enclosed in a glass tube. A fritted glass filter near the lower end of the tube caused the pure N_2 entering at the bottom to be divided into very small bubbles which swept through the liquid carrying along the oxygen produced there. By switching the gas current from O to S the nitrogen could be admitted into the phosphor chamber P without passing through O. If, as in our experiments, O contains an aqueous solution a third liquid nitrogen trap T_3 must be inserted between O and P because of the harmful action of water vapor on the phosphor.[2]

The phosphor P* fills one side of a vertical U-tube of 6-mm diameter to a height of about 5 cm and is held in place by nickel gauze plugs. The U-tube is closed on both ends by stopcocks, one connecting it with O, the other with a mercury vapor pump and an outlet A_2 into the atmosphere. U, S, and K are fixed to the system with standard ground joints so that they can be easily taken apart to renew the phosphor or the potassium or to clean the intermediate tubing.

The U-tube containing the phosphor is placed between the disks of a Becquerel phosphoroscope having an aperture of 180° in the disk on the side of the exciting light and of 30° in the other disk. The exciting light is produced by a 6-volt 108-w projection lamp, and after passing through a system of lenses is reflected at 90° by a prism inside the phosphoroscope so that it strikes P at a grazing angle on the side from which the phosphorescence is observed. The diameter of the luminescent image is about 3 mm. The phosphorescent light passes through a lens of short focal length into a photo-tube of the electron multiplier type (RCA 931).* The amplified current is measured with a Rubicon galvanometer of sensitivity 4×10^{-9} amp./mm. The inertia of the instrument is sufficient so that the deflection remains fairly steady if the phosphoroscope has a rotational frequency of 6 per second.

At the beginning of an experiment, the evacuated line is filled with pure N_2, the final step being the admission of the N_2 into the phosphor chamber. If the phosphorescence intensity is not diminished from its value in vacuum, the N_2

* The method of preparing the phosphor has been described in the paper mentioned in references 1 and 2. It has been ascertained in the meantime, that the initial purification of the gel is carried out with better results by washing the gel for several days with hydrochloric acid and subsequently with distilled water, instead of following Kautsky's method of using sulfuric acid and, after rinsing the gel with water, neutralizing with ammonia.

* If no electron multiplier tube is available a photo-cell with electrometer or some amplifying device can be used. If the variations in O_2 production are rapid, the electrometer has the disadvantage that an inertia is introduced by the time required to charge it to a certain voltage.

stream is sufficiently pure for proceeding with the experiment. The U-tube containing the phosphor is closed off, and the gas stream is made to pass through O which it flushes for several hours, the gas finally escaping at A_1. (Whenever a measurement is to be made the gas stream is again made to pass through the phosphor.) The rate of flow must be so chosen so that certain difficulties are avoided. If it is too rapid as compared with the rate of oxygen production the concentration of O_2 in the gas reaching the phosphor is too low and makes the quenching action very small; furthermore, too strong a current is apt to carry water droplets from O into T_3, blocking the tube. If, on the other hand, the flow is too slow so that the oxygen in contact with the phosphor is not quickly removed, an appreciable part of the oxygen is consumed by interaction with the dye and the calibration of the phosphor which is valid for constant O_2 pressures can no longer be applied.

A variation in the rate of flow does not affect the time scale of the curve representing the phosphorescence intensity as a function of time. If the gas is carried from O to P in a time ϑ, events occurring in O at t_1 and t_2 are recorded by the phosphoroscope at times $t_1+\vartheta$ and $t_2+\vartheta$, so that the interval t_2-t_1 remains unaltered. On the other hand, the flow rate influences the resolving power of the method. With a slow gas current two events which are separated in O by a short interval Δt will overlap in their effects on the phosphor and all finer details will be blurred out more or less. It is favorable therefore to make the rate of flow as large as is compatible with the rate of oxygen production and the sensitivity of the phosphor.

Furthermore, it is desirable to render the time lag ϑ as short as possible by reducing the volume of the tubing connecting O and P. The minimum length of this tubing is determined by the necessity of inserting a liquid air trap and a number of stopcocks while the phosphor must be placed inside of the phosphoroscope. If the total length is of the order of magnitude of 100 cm and the rate of flow is 3 cc/minute, ϑ is of the order of 10 minutes if the tubes have an average diameter of 6 mm; if these tubes are replaced by capillaries with a diameter of 1 mm ϑ is reduced to less than 20 sec. The constancy of ϑ which can be measured very accurately provides a check for the constancy of the flow rate (see Fig. 5). In our experiments a flow rate of 3 cc per minute proved to be of the right order of magnitude. It was adjusted by means of two valves in series at the outlet of the N_2 cylinder and was controlled by a bubble counter at A_2. Since the luminescent spot has a height of only 3 mm the streaming gas was in contact with the excited dye molecules for only a fraction of a second and this is not sufficient for an appreciable part of the oxygen to be consumed.

After the phosphor has been irradiated many hours in the presence of O_2 the illuminated spot begins to be discolored and the phosphorescence deteriorates. Therefore the phosphoroscope is so constructed that its height can be varied with respect to the U-tube and a fresh spot of the phosphor can be used. After a series of measurements a small amount of oxygen remains adsorbed on the gel. In order to minimize deterioration of the phosphor by this oxygen, it was found advantageous to pump out the U-tube and to keep it connected with the mercury vapor pump at all times when an experiment is not in progress. With these provisions the phosphor filling need not be renewed for a period of several months without losing its full sensitivity.

The sensitivity of the phosphor to quenching by oxygen has been measured by admitting small quantities of air into the phosphor chamber, measuring the pressure with a McLeod gauge, and noting the corresponding phosphorescence intensity. Such a calibration has of course to be renewed for every fresh phosphor and must be repeated from time to time for the same one. Furthermore, it had to be ascertained whether this calibration still holds when the same quantity of oxygen is contained in nitrogen of atmospheric pressure. In order to obtain a calibration under conditions closely approaching those of the measuring experiments, the oxygen source O was replaced by a vessel having the form of a mercury vapor trap and containing glass beads dusted with mercuric oxide powder. Since the dissociation pressure of HgO is known for various temperatures[4] the oxygen pressure in the vessel could be kept at various values with appropriate temperature baths. At the slow rate of gas flow it could

[4] G. B. Taylor and G. A. Hulett, J. Phys. Chem. **17**, 588 (1913).

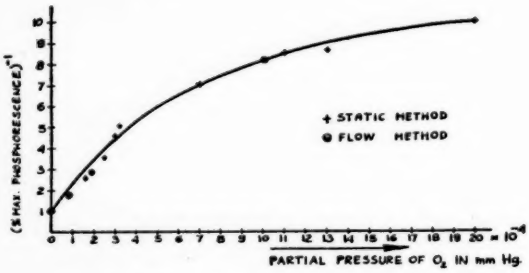

FIG. 2. Calibration of gel phosphorescence.

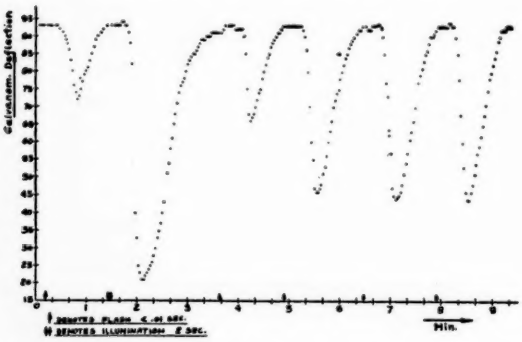

FIG. 3. Quenching of phosphorescence caused by photosynthetic production of oxygen in algae illuminated by flashes of light.

be assumed that after passing through the tightly packed glass beads the nitrogen was saturated with O_2 of the pressure corresponding to the temperature. In Fig. 2 the crosses refer to the calibration of the phosphor with air of low pressure, the circles to the calibration with oxygen in one atmosphere of nitrogen. Since both series of points fall on a fairly smooth curve the first method, which is the easier, can be applied in general.

Figure 3 is a sample experimental curve showing the quenching effect of oxygen produced in a suspension of algae illuminated by light flashes. A decrease in phosphorescence intensity corresponds to an increase in oxygen content of the gas. The second strong minimum of the curve is caused by an illumination lasting two seconds; the other minima correspond to light outbursts of photographic flash bulbs, lasting only about 3×10^{-2} second. The difference in depth of the various minima is real, but will not be discussed here since it is due to the biochemical behavior of the algae.

The figure shows the limitation of the method with respect to an exact reproduction of the rate of oxygen development. If the rate of flow was correctly adjusted to 3 cc per minute in our set-up, 20 seconds elapsed between the start of the illumination and the initial decrease of phosphorescence. Superimposed on this time lag, which causes only a shift of the curve along the time axis, is a real distortion of the curve due to the fact that not all of the oxygen produced at a given moment is instantaneously flushed out by the current. Figure 3 shows that the effect of the practically timeless light flash is spread over about 60 seconds; that of the 2 seconds illumination is drawn out to 2 minutes. This evidently is caused not by the unequal length of illumination periods, since either one is short compared to a minute, but rather by the difference in the quantity of oxygen that must be driven out of the water. The distortion becomes greater if the oxygen production is larger and lasts longer. After an oxygen production lasting ten minutes, during which time the phosphorescence is severely quenched, it requires 5 to 15 minutes for the phosphor to regain its full intensity. That this is due not to an inertia of the phosphor but to the time needed to flush all the O_2 out of the water is proved by the fact that as soon as the gas current is directed through *S* instead of *O* the full phosphorescence is restored almost immediately.

By means of the calibration curve of Fig. 2 the directly measured phosphorescence intensities

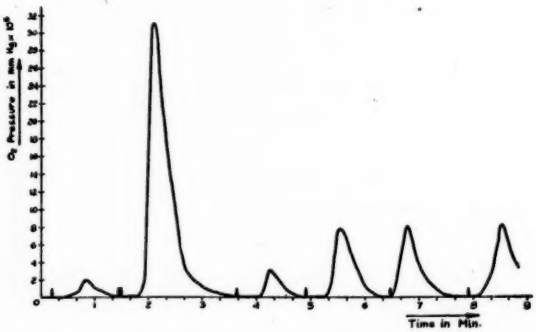

FIG. 4. The data from Fig. 3 converted into oxygen pressure.

plotted in Fig. 3 can be converted into the corresponding oxygen pressures; the converted curve is shown in Fig. 4. The total quantity of oxygen produced by a single light flash can be computed by integrating over the surface cut out by the

oxygen pressure curve for the corresponding time period. If the rate of flow is 3 cc per minute, the number of oxygen molecules produced by a light flash is given by

$$n = \tau \bar{p}/760 \cdot 3N,$$

where $\bar{p}$ is the average oxygen pressure observed during the time τ (τ measured in minutes); N is the number of molecules in 1 cc of perfect gas at standard conditions ($N = 2.7 \times 10^{19}$). The number of O_2 molecules produced by the light flash of Fig. 4 is thus computed to be $n = 4 \times 10^{12}$. If the oxygen production is so large that the phosphorescence recovers only slowly, the calculation of the amount of oxygen produced at every moment becomes less exact. Some of the oxygen has been retained in the water and quenches the phosphorescence after the end of the oxygen production period; it is not possible to ascertain when this oxygen has actually been produced. Nevertheless any change in the rate of oxygen development during this period shows up as a change in slope of the phosphorescence intensity curve and the end of the period is determined with the same exactitude and has the same time lag ϑ as the beginning. This is shown in Fig. 5 which represents the oxygen production of a solution of algae illuminated continuously for six minutes. The biological interpretation of the curves in Figs. 3–5, which are reproduced here only as examples for the application of the method, will be discussed elsewhere.

Figure 6 illustrates the application of the method in a field which is not connected with biochemistry, namely, the measurement of the oxygen production by electrolysis in the potential range in which the "residual current" gives way to the normal current. Curve *1* gives the galvanometer deflections corresponding to decrease in photoelectric currents. Curve *2* gives these readings converted into O_2 pressures (left-hand scale) or number of O_2 molecules produced per second (right-hand scale); and curve *3* gives the electrolytic currents—all as functions of applied voltage. The cell, of the same design as that used in the work with algae, was fitted with platinum wire electrodes and contained distilled water slightly acidified with H_2SO_4. The sharp onset of the oxygen production at a voltage between 1.5 and 1.6 volts (twice repeated) is even more

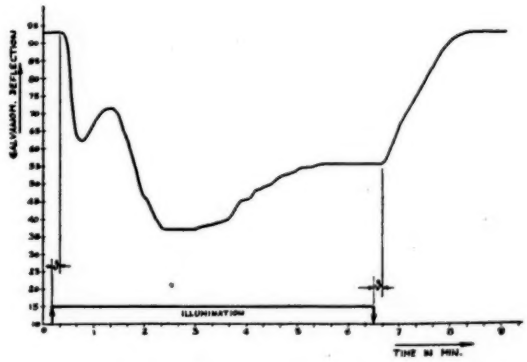

FIG. 5. Variation of oxygen production by algae under constant illumination in the absence of CO_2.

obvious in the direct readings of curve *1* than in the converted curve *2*, because the method has its highest sensitivity for small O_2 pressures. On the other hand, the conversion of the highest points of curve *1* yields less reliable results. If one computes the oxygen yield according to Faraday's law from the current values of curve *3*, it is seen

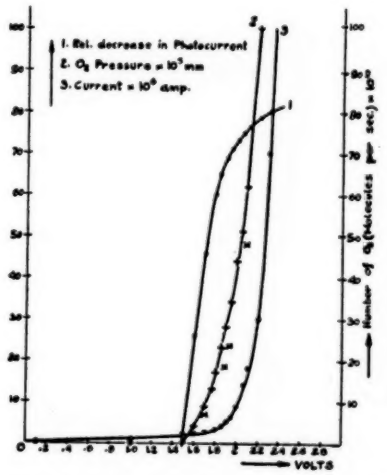

FIG. 6. Oxygen production by electrolysis.

that the first points of curve *2* correspond to an O_2 production which is of the order of 0.1 percent of the calculated value; at the highest point of curve *2*, the O_2 production has already increased to 10 percent of this value. These results agree in principle with those obtained by other means, but by any other method it would be difficult to determine with equal precision the point at which the oxygen production sets in and which corresponds to the decomposition voltage.

The Vibrational Spectrum of Pyridine and the Thermodynamic Properties of Pyridine Vapors

CHARLES H. KLINE, JR.,* AND JOHN TURKEVICH
Frick Chemical Laboratory, Princeton University, Princeton, New Jersey

(Received March 27, 1944)

An analysis of the vibrations of the pyridine molecule was made on the basis of infra-red, Raman, and ultraviolet absorption spectra. The fundamental frequencies were assigned and the thermodynamic properties of pyridine were calculated on the basis of such an assignment.

IN connection with catalytic studies on the synthesis of pyridine the thermodynamic properties of pyridine vapors at elevated temperatures were desired. As no experimental data are available, the required functions were calculated by statistical methods. Application of these methods required the determination of the fundamental frequencies in the vibrational spectrum of pyridine.

The observed vibrational spectrum of pyridine has frequently been recorded. The data available on pyridine and the recent thorough investigations on the closely related benzene spectrum[1–4] make possible a reasonably satisfactory analysis of the pyridine spectrum which is sufficiently accurate for the required statistical calculations.

Of the numerous investigations of the Raman spectrum of pyridine[5–17] those of Venkateswaran,[5,9,13] Krishnamurti,[11] Kohlrausch,[14,15,18] and Ananthakrishnan[16] are the most accurate and extensive. The results of these investigators are given in the first four columns of Table I, which summarizes the observed lines in the pyridine spectrum and their assignments. Only three lines have been reported which were not found by these four investigators; these lines have no significance and appear to have been caused by impurities in the samples or to errors. The three lines are given in column five of Table I.

Henri and Angenot[19] have analyzed the vibrational fine structure of the ultraviolet absorption spectrum of pyridine. The vibrational frequencies found by them are given in column six of Table I.

The infra-red absorption spectrum of liquid pyridine has been investigated three times in the region beyond 3μ, which contains all the fundamentals.[20–22] The infra-red absorption spectrum of pyridine vapor has recently been measured by Turkevich and Stevenson.[23] As the pyridine used by the earlier investigators appears to have been contaminated with α-picoline, the sample used by Turkevich and Stevenson was taken from a narrow-cut commercial pyridine and purified by three crystallizations of the pyridine—zinc-chloride double salt from absolute alcohol. This pyridine should therefore have been free of homologs and other impurities.[24] The results of the infra-red investigations appear in columns seven to ten of Table I.

* Now Ensign, USNR.

[1] Lord and Andrews, J. Phys. Chem. **41**, 149–158 (1937).
[2] Angus, Bailey, Ingold, Wilson, *et al.*, J. Chem. Soc., pp. 912–987 (1936).
[3] Langseth and Lord, Kgl. Danske Vid. Sels. Math.-Fys. Medd. **16**, No. 6, 85 pp. (1938).
[4] K. S. Pitzer and Scott, J. Am. Chem. Soc. **65**, 803–829 (1943).
[5] Ganesan and Venkateswaran, Ind. J. Phys. **4**, 195–280 (1929).
[6] Ôkubo and Hamada, Sci. Rep. Tôhoku Imp. Univ. [I], **18**, 601–608 (1929).
[7] Petrikaln and Hochberg, Zeits f. physik. Chemie **B3**, 217–228, 405 (1929).
[8] Bonino and Brüll, Gazz. Chim. Ital. **59**, 675–680 (1929).
[9] Venkateswaran, J. Phys. Chem. **34**, 145–152 (1930).
[10] C. E. Cleeton and R. T. Dufford, Phys. Rev. **37**, 362–372 (1931).
[11] Krishnamurti, Ind. J. Phys. **6**, 367–387 (1931).
[12] Whiting and Martin, Trans. Roy. Soc. Canada [III], **25**, Sec. 3, 87–98 (1931).
[13] Venkateswaran, Phil. Mag. **15**, 263 (1933).
[14] Kohlrausch and Pongratz, Ber. **B67**, 1474 (1934).
[15] Kohlrausch, Zeits. f. physik. Chemie **B30**, 315 (1935).
[16] Ananthakrishnan, Proc. Ind. Acad. Sci. **A3**, 52–74 (1936).
[17] Bernstein and Martin, Trans. Roy. Soc. Canada [III], **31**, 95–103 (1937).
[18] Herz, Kahovec, and Kohlrausch, Zeits. f. physik. Chemie **B53**, 124–148 (1943).
[19] Henri and Angenot, Comptes rendus **201**, 895–896 (1935); J. chim. phys. **33**, 641–665 (1936).
[20] Coblentz, *Investigations of Infra-Red Spectra* (Washington, D. C., Carnegie Institute, 1905), Part I, pp. 96, 145, 272, 274, and insets.
[21] Spence, Astrophys. J. **39**, 243–263 (1914).
[22] Lecomte, Comptes rendus **207**, 395–398 (1938).
[23] J. Turkevich and P. C. Stevenson, J. Chem. Phys. **11**, 328–9 (1943).
[24] Heap, Jones, and Speakman, J. Am. Chem. Soc. **43**, 1936–1940 (1921); Mahan and Bailey, *ibid.* **59**, 2449–2450 (1937).

Column eleven gives averages for the observed lines. Columns twelve, thirteen, and fourteen give the depolarization factors for certain of the Raman lines as determined by Venkateswaran,[13] A. W. Reitz (reported in reference 18), and Kohlrausch,[18] respectively.

ANALYSIS OF THE SPECTRUM

The similarity of the spectra of benzene and pyridine has been remarked by a number of authors.[5, 9, 10, 13, 15, 18, 19, 22] Depolarizations of the principal corresponding Raman lines are practically identical.[13] The chemical similarity between benzene and pyridine is well known, and electron-diffraction data[25] show that the structures of the two molecules differ only negligibly.

The following discussion will show that the ring vibrations of pyridine parallel those of benzene and can be readily located; the hydrogen vibrations of pyridine show considerable divergence from those of benzene and can only be tentatively assigned.

Normal Modes of Vibration of Pyridine

The symmetry of pyridine is C_{2v}. This is the symmetry that results by replacing one $-CH$ group in benzene by a nitrogen atom; it is the symmetry of monodeuterobenzene[3] and of pyrrole.[26] No higher symmetry is compatible with the established chemical structure of the molecule. Lower symmetries are improbable: A C_1 symmetry can at once be excluded, for it would require that all the Raman lines be polarized; a symmetry C_s, requiring that the molecule have only one vertical plane of symmetry, can be ruled out, as this would require that the molecule be aplanar or that it be planar but unsymmetrical, as if it were frozen into one of the two Kekulé resonance forms, for example.

Given a symmetry C_{2v}, we readily find the distribution of the twenty-seven fundamental frequencies into the four symmetry classes either by group theory[27] or the equivalent symmetry theory.[28] Table II gives the various classes and the selection rules. In deriving Table II the two-fold rotational axis of symmetry through the nitrogen atom and the gamma-carbon atom is taken as the z axis. The x axis lies in the plane of the molecule; it is perpendicular to the z axis, which it intersects at the center of gravity of the molecule. The y axis is perpendicular to the plane of the molecule and intersects the x and z axes at the center of gravity.

As pyridine differs but little from benzene and as the observed pyridine spectrum is very similar to that of benzene, the normal modes of vibration of the two molecules must also be very similar. The normal modes of vibration of benzene have been calculated by the methods of group theory by Wilson;[29] they are shown schematically in Fig. 1, as given by Langseth and Lord.[3] The low symmetry of pyridine makes such a calculation prohibitively laborious. The normal modes of pyridine, however, may as a first approximation be taken as those of benzene, except that three hydrogen vibrations (one stretching and two bending) will be lacking in pyridine.

Table III shows the changes in the symmetry classes on transition from a D_{6h} structure in benzene to a C_{2v} structure as in monodeuterobenzene and further to the C_{2v} structure of pyridine. Note that in Table III the translational and rotational motions are referred to different axes in the D_{6h} and C_{2v} structures.

On passing from a monosubstituted benzene (such as monodeuterobenzene) to pyridine a hydrogen stretching frequency disappears from class A_1, a planar hydrogen bending frequency from class B_1, and an out-of-plane hydrogen bending frequency from class B_2. As the schematic vibration diagrams of Fig. 1 have no more than a qualitative significance for pyridine, it is highly arbitrary to speak of omitting any three specific vibrations; for convenience, however, the pyridine vibrations have been numbered according to the more or less analagous benzene vibrations, and vibrations $7a$, $9b$, and $17b$ have been omitted. It must be realized that this is only a matter of expediency.

---

[25] Schomaker and Pauling, J. Am. Chem. Soc. **61**, 1769 (1939).
[26] R. C. Lord, Jr., and F. A. Miller, J. Chem. Phys. **10**, 328–341 (1942).
[27] Rosenthal and Murphy, Rev. Mod. Phys. **8**, 317 (1936).
[28] Kohlrausch, *Der Smekal-Raman Effekt. Ergänzungsband* (Julius Springer, Berlin, 1938), p. 44.
[29] E. B. Wilson, Jr., Phys. Rev. **45**, 706 (1934).

TABLE I. The vibrational spectrum of pyridine.

1	2	3	4	5	6	7	8	9	10	11	12	13	14	15
	Raman spectrum (liquid)				UV (vap.)	Infra-red (liquid)			IR (vap.)	Av.	Depolarization			Assignment
Venkat.	Krish.	Kohlr.	Ananth.	Others	H & A	Coblentz	Spence	Lecomte	T & S		Venk.	Reitz	Kohl.	(Fundamentals are underlined and starred)
				216 (2)[a]						216				Picoline
	371 (0)	374 (00)	377 (0)							374				*16b
405 (1)	403.6 (1)	405 (1)	402 (1)							404			0.72	*16a
				472 (3)[b]						472				Error
	553 (0)?		553 (0)							553				Picoline
603 (1)	603 (1½)	605 (3)	602 (1)		600			601 s	610 m	604	0.7	dp	0.73	**6a, 6b
									630 m	630				1028 −404 =624; 1037 −404 =633
651 (2)	651.9 (3)	652 (5)	652 (3)						650 m	652	0.8	dp	0.76	*4
									{662 669 s 690}	669				*11
	717 (0)	710 (0)				709 (10)		708 s	710 m	710				*10b
	747 (0)	749 (0)				751 (7)		746 s	744 w	747				*10a
									763 w	763				374 +404 =778
									795 w	795				2 ×404 =808
	806 (0)	812 (0)	799 (0)			806 (1)		811 w		807				Picoline; 2 ×404 ??
						840 (½)			833 w	836				1210 −374 =836 ?? 1440 −604 =836 ??
						855 (½)			847 w	850				1570 −710 =860 ??
884 (1)	885 (1)	886 (1)	878 (½)		857	886 (1)		890 w	881 w	884		(0.50)	(0.42)	*18a
						922 (½)			907 w	915				1570 −652 =918 ?
935 (0)	942 (0)	942 (0) ?	942 (0)			949 (½)			936 m	941				*5
		980 (2)	979 (0)							980				1580 −604 =976 See text.
988 (10)	992 (10)	990 (10)	990 (10)		993	992 (5½)	985 s	984 s		990	0.1	0.04	0.05	*1
1027 (10)	1029.4 (10)	1029 (10)	1028 (10)		1031	1028 (4½)	1023 s	1020 s		1028	0.2	0.04	0.05	*12
		1043 (0)	1040 (0)			Shoulder			1037 s	1037				*18b
		1054 (0) ?								1054				Picoline
	1067 (1)	1069 (1)	1057 (0)			1069 (3½)	1053 m	1052 w		1061				*17a
1157 (1)	1145 (1)	1144 (0)	1143 (½)		1159	1138 (3)	1137 m	1125 w	1136 w	1139		0.67	0.76	**9a, 15
									1156 w	1156				404 +747 =1151 ?
1217 (2)	1218 (3)	1218 (5)	1218 (3)			1211 (2½)	1202 m	1190 w	1202 w	1210	0.6	0.75	0.72	*3
				1268 (1)[b]					1263 w	1265				Picoline; 604 +652 =1256; 604 +669 =1273
						1290 (½)				1290				2 ×652 =1304

TABLE I.—*Continued.*

1	2	3	4	5	6	7	8	9	10	11	12	13	14	15
	Raman spectrum (liquid)				UV (vap.)	Infra-red (liquid)			IR (vap.)	Av.	Depolarization			Assignment
Venkat.	Krish.	Kohlr.	Ananth.	Others	H & A	Coblentz	Spence	Lecomte	T & S		Venk.	Reitz	Kohl.	(Fundamentals are underlined and starred)
1376 (1)						1369 (1)			1376 w	1374				990+374=1364; Picoline?
	1439 (0)	1438 (1)	1444 (0)			1439 (6)	1438 s		1445 s	1440				*19b
1486 (0)	1483 (1½)	1480 (3)	1485 (1)			1481 (5)			{1481 1510 s}	1485		p?	p	*19a
1576 (3)	{1571.4 (4) 1580.8 (2)	1570 (5) 1580 (5)	1570 (2) 1579 (2)				}1574 s{			1570 1580	0.8	dp	0.71	*8b *8a
	1596.7 (1)	1596 (2)	1594 (1)			1600 (5½)			1605 s	1598				990+604=1594 See text.
						1723 (1)				1723				*14
									1830 m	1830				884+941=1825 See text.
						1923 (1*B*)	1915 w			1920				990+941=1931
									1991 m	1991				941+1061=2002 See text.
	2368 (½)	2368 (0) ?	2370 (0)							2369				1485+884=2369 ??
	2455 (½)	2451 (0)	2449 (0)							2452				1440+1028=2468 ??
	2651 (0)	2651 (0) ?	2658 (0)							2653				1440+1210=2650 ??
	2867 (½)	2868 (1)	2871 (0)							2869				2×1440=2880 ??
	2913 (½)	2911 (1)	2908 (0)							2911				Picoline; 1440+1485=2925 ??
	2952.2 (1)	2952 (1)	2951 (1)							2952				2×1485=2970 ??
	2985 (½)	2988 (1)	2986 (0)							2986				
	3024 (1)	3023 (1)	3025 (½)							3024				1440+1570=3010 ?
3033		3031 (0)	3034 (½)							3033	0.8			1440+1580=3020 ?
3056 (8)	3054 (10)[c]	3054 (5*B*)	3054 (8*B*)							3054	0.4		0.36	***2, 13, 7b (1485+1570=3055)
		3069 (0)	3063 (½)							3066				1485+1580=3065 ?
	3089 (½)	3090 (0)	3090 (½)			3076 (3½*B*)	3076 m		3070 s	3075				**20a, 20b
	3144.1 (1½)	3143 (1)	3142 (1½)							3143				2×1570=3140 ?
	3175 (½)	3175 (1)	3172 (½)							3174				2×1580=3160 ?

Notes: All frequencies are given in cm^{-1}. Kohlrausch's intensities and those of column 5 have been adjusted to the basis of an intensity 10 for the 990-cm^{-1} line.

Symbols and abbreviations:

a, Bonino and Brüll, reference 8, observers.
b, Bernstein and Martin, reference 17, observers.
c, Line reported as having "rotational wings."
B, Broad line.
?, Question mark indicates uncertainty on the part of the authors whose results or proposals are recorded in the column where datum is questioned. In column 15, ? and ?? indicate uncertain and very uncertain assignment by the authors of the present paper.

s, Strong line.
m, Medium line.
w, Weak line.

p, Polarized line.
dp, Depolarized line.

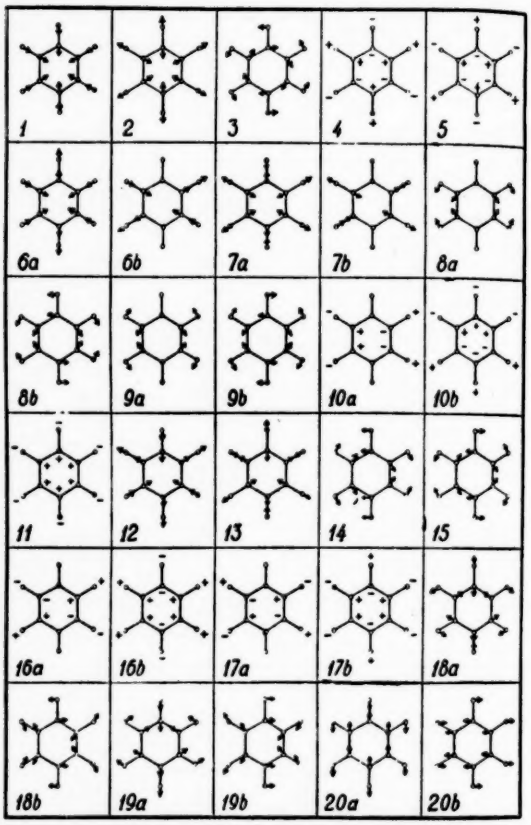

FIG. 1. Normal modes of vibration of benzene (Langseth and Lord, after Wilson). The two components of each degenerate vibration are denoted by *a* and *b*. Component *a* is symmetrical to a twofold axis through the para carbon atoms, and component *b* asymmetrical.

Ring Vibrations

Transition from a D_{6h} to a C_{2v} structure in benzene and related compounds releases the degeneracy of the ten degenerate benzene vibrations, and each degenerate frequency is split into two components, one symmetrical and one asymmetrical to the C_2^z axis. In monodeuterobenzene the degenerate vibrations of the carbon ring of benzene appear as doublets with a separation of 3.5 to 55 cm^{-1}. In Table IV the ring vibrations of benzene are given as well as the corresponding vibrations of monodeuterobenzene and the ring vibrations of pyridine as proposed in the present paper.

The great similarity of the three ring-vibration spectra of Table IV is very convincing evidence for the frequencies assigned to the ring vibrations of pyridine. The following detailed consideration of the individual lines lends considerable support to the assignment.

$\nu 16a$ and $\nu 16b$ at 374 and 404 cm^{-1} are both weak in the Raman spectrum of pyridine, as in the deuterated benzenes.

$\nu 6a$ and $\nu 6b$ are both assigned to 604 cm^{-1}. These frequencies are similarly unresolved in the spectra of several of the deuterobenzenes. The occurrence of the 604-cm^{-1} line in the ultraviolet

TABLE II. Selection rules for pyridine (symmetry C_{2v}).

	Essential symmetry elements			Selection rules			Vibrations		
Class	C_2^z	σ_x	σ_y	Raman	I.R.	Trans. & Rot.	Ring	Hyd.	Total
A_1	*s*	*s*	*s*	*p*	*a*	T_z	5	5	10
A_2	*s*	*as*	*as*	*dp*	*ia*	R_z	1	2	3
B_1	*as*	*as*	*s*	*dp*	*a*	T_x, R_y	4	5	9
B_2	*as*	*s*	*as*	*dp*	*a*	T_y, R_x	2	3	5

TABLE III. Symmetry classes for benzene, monosubstituted benzenes, and pyridine.

Benzene	Monosubstituted benzene	Pyridine
A_{1g} (−, −): 1, 2		
B_{1u} (−, −): 12, 13		
	A_1 (*R*, *IR*): 1, 2, 6*a*, 7*a*, 8*a*, 9*a*, 12, 13, 18*a*, 19*a*, 20*a*, T_z	A_1 (*R*, *IR*): 1, 2, 6*a*, —, 8*a*, 9*a*, 12, 13, 18*a*, 19*a*, 20*a*, T_z
E_g+ (*R*, −): 6, 7, 8, 9		
E_u− (−, *IR*): 18, 19, 20, T_x, T_y		
	B_1 (*R*, *IR*): 3, 6*b*, 7*b*, 8*b*, 9*b*, 14, 15, 18*b*, 19*b*, 20*b*, T_x, R_y	B_1 (*R*, *IR*): 3, 6*b*, 7*b*, 8*b*, —, 14, 15, 18*b*, 19*b*, 20*b*, T_x, R_y
B_{2u} (−, −): 14, 15		
A_{2g} (−, −): 3, R_z		
B_{2g} (−, −): 4, 5		
A_{2u} (−, *IR*): 11, T_z		
	B_2 (*R*, *IR*): 4, 5, 10*b*, 11, 16*b*, 17*b*, T_y, R_x	B_2 (*R*, *IR*): 4, 5, 10*b*, 11, 16*b*, —, T_y, R_x
E_u+ (−, −): 16, 17		
E_g− (*R*, −): 10, R_x, R_y		
	A_2 (*R*, −): 10*a*, 16*a*, 17*a*, R_z	A_2 (*R*, −): 10*a*, 16*a*, 17*a*, R_z

vibrational spectrum shows that there must be a totally symmetric vibration of this frequency. The high depolarization factor of the Raman line may result from the coincidence of the non-totally symmetric vibration $\nu 6b$.

The exact location of $\nu 4$ in benzene is in some doubt: Langseth and Lord estimate it to be at 664 cm^{-1} by the product rule, and Pitzer and Scott have assigned it to the weak Raman line appearing in violation of the selection rules at 685 cm^{-1} in liquid benzene. In pyridine $\nu 4$ is probably the rather strong Raman line at 652 cm^{-1}. This frequency appears too intense to be correlated with the powerful infra-red line at 669 cm^{-1}. Furthermore, this infra-red line has a pronounced shoulder at about 650 cm^{-1}, which argues for the existence of an independent line at this point. $\nu 4$ is allowed in both infra-red and Raman spectra in pyridine.

$\nu 1$ and $\nu 12$, the powerfully polarized Raman lines at 990 and 1028 cm^{-1}, both fall in the same symmetry class in pyridine and by the customary interaction are displaced away from each other appreciably more than in benzene. The separation between $\nu 1$ and $\nu 12$ is 18 cm^{-1} in benzene, 28 cm^{-1} in monodeuterobenzene, and 38 cm^{-1} in pyridine. The complete absence of $\nu 1$ from the infra-red spectrum of pyridine vapor is interesting in view of the intensity of this line in the infra-red spectrum of the liquid. $\nu 1$ is forbidden by symmetry in the infra-red spectrum of benzene vapor but may be the line appearing in the liquid at about 985 cm^{-1} as a shoulder on the strong line at 1033 cm^{-1}. The absence of $\nu 1$ from the infra-red spectrum of pyridine vapor illustrates very strikingly the manner in which pyridine behaves almost as if it had the D_{6h} symmetry of benzene.

$\nu 19b$ and $\nu 19a$ are assigned to 1440 and 1485 cm^{-1}, respectively, in pyridine. The line at 1485 cm^{-1} appears as a doublet in the infra-red spectrum of pyridine vapor, the two components being located at 1481 and 1510 cm^{-1}. This doublet probably represents the imperfectly resolved P and R branches; the observed separation of 29 cm^{-1} is not far from the separation of 23 cm^{-1} found between the P and R branches of the 1485-cm^{-1} line of benzene in the more accurate measurements of Bailey, Hale, Ingold, and Thompson.[2] Assignment of the totally symmetric $\nu 19a$ to 1485 cm^{-1} rather than to 1440 cm^{-1} is supported by the depolarization data and the greater intensity of the 1485 cm^{-1} Raman line.

TABLE IV. Ring vibrations of benzene, monodeuterobenzene, and pyridine.

Vibration	Benzene		Monodeutero-benzene	Pyridine
	L&L	P&S	L&L	
$16b$	406		381	374
$16a$			403	404
$6a$	606.4		598.5	604[a]
$6b$			602.0	604[a]
4	664[b]	685[c]	—	652
1	992.5		980.9	990
12	1010[b]		1008.6	1028
$19b$	1485		1418 ??	1440
$19a$			1473[b]	1485
$8b$	1595		1575.7	1570
$8a$			1593.8	1580
14	*d*	1693[c]	—	1723

Notes: Frequencies in cm^{-1}.
L&L, Langseth and Lord, reference 3.
P&S, Pitzer and Scott, reference 4.
a, component of an unresolved doublet.
b, calculated from Teller's product rule.
c, appears in the Raman spectrum of liquid benzene although forbidden by the selection rules.
d, Lord and Andrews (reference 1) calculate 1854 cm^{-1}.
??, assignment considered doubtful by Langseth and Lord.

Release of the degeneracy of $\nu 8$ in benzene (at 1595 cm^{-1}) on transition to pyridine gives a difficultly resolvable doublet at 1570 and 1580 cm^{-1}. In benzene there is also another rather strong line at 1604 cm^{-1} representing the combination $\nu 1+\nu 6$, which is much stronger in the Raman spectra than is customary for combination tones because of resonance with $\nu 8$. A similar situation occurs in pyridine, where besides the $\nu 8a$, $\nu 8b$ doublet there occurs a strong Raman line at 1598 cm^{-1} representing $\nu 1+\nu 6$. Resonance between $\nu 1+\nu 6$ and $\nu 8$ has the further effect of causing a satellite to $\nu 1$ to appear in the pyridine spectrum at 980 cm^{-1} similar to the satellites at 979.6 and 999.0 cm^{-1} in benzene. Because of the resonance between $\nu 8$ and $\nu 1+\nu 6$ and the consequent mixing of the wave functions a vibrational transition from the first excited level of $\nu 6$ to either the $\nu 8b$ (1580 cm^{-1}) or $\nu 1+\nu 6$ (1598 cm^{-1}) lines gives rise to Raman scattering differing but little (except in intensity) from the scattering caused by transition of $\nu 1$ from the ground state

to the first excited state. Two satellites to the 990-cm^{-1} line ($\nu 1$) should therefore be found at $1580-604=976$ cm^{-1} and $1598-604=994$ cm^{-1}. The faint Raman line at 980 cm^{-1} in pyridine may be taken as the first difference; the second satellite is extremely weak in benzene and has doubtless not been observed in pyridine because of the nearness to 990 and 1028 cm^{-1}. The two remaining satellites to $\nu 1$ in benzene (at 984 and 1005 cm^{-1}) arise from isotopic impurity, about 6 carbon atoms in every 100 being C^{13}. In pyridine C^{13} substitution can occur in three non-equivalent positions in the ring, and isotopic satellites to the different lines are doubtless too weak ever to be observed.

$\nu 14$ has never been definitely located in benzene, where the vibration is forbidden in both Raman and infra-red spectra. Lord and Andrews[1] calculated from Wilson's force constants the value $\nu 14=1854$ cm^{-1}. Angus *et al.* calculated[2] $\nu 14=1720$ cm^{-1}. From consideration of the other planar carbon bending frequencies Langseth and Lord[3] estimated that $\nu 14$ lies in the region 1440–1900 cm^{-1}. Pitzer and Scott[4] have chosen the weak Raman line at 1693 cm^{-1} to represent this vibration, on the assumption that this line appearing in the spectrum of this liquid may represent a forbidden line because of the relaxation of the selection rules in the liquid state.

In pyridine there are four possibilities for $\nu 14$, the two infra-red lines of the liquid at 1723 and 1920 cm^{-1} and the two infra-red lines of the vapor at 1830 and 1991 cm^{-1}. Because of the close similarity in the vapor-phase spectra of pyridine and benzene it seems unlikely that either of the vapor lines represents $\nu 14$. Furthermore these two lines are very similar to the lines in benzene vapor at 1808 and 1961 cm^{-1}, which Pitzer and Scott explain as the allowed combinations $\nu 10+\nu 17$ and $\nu 5+\nu 17$, respectively. The pyridine lines can also be assigned to these combinations on the basis of the assignment of fundamentals proposed here. Of the two lines in the liquid that at 1920 cm^{-1} lies somewhat too high for a ring vibration, and $\nu 14$ has therefore tentatively been assigned to 1723 cm^{-1}. In any event this cannot be far wrong.

The Hydrogen Vibrations

Although the ring vibrations of pyridine can be elucidated in a reasonably satisfactory manner, the hydrogen vibrations can be located only in an approximate fashion. There appear to be differences in the force-constants of some of the pyridine vibrations as compared with the similar benzene vibrations. Thus, for example, attempts to locate the hydrogen frequencies of pyridine between the hydrogen frequencies of equivalent symmetry in benzene fail although a well-known theorem in dynamics states that if a system loses one degree of freedom then the $(s-1)$ new frequencies lie in the intervals between the s frequencies of the original system.

In general, transition from benzene to pyridine causes a displacement of the hydrogen frequencies toward lower frequencies; this is especially marked in some of the bending vibrations.

Class A_1

This class includes the totally symmetric vibrations; the frequencies are allowed in both Raman and infra-red spectra and appear in the ultraviolet vibrational spectrum. The ring frequencies are $\nu 1$, $\nu 6a$, $\nu 8a$, $\nu 12$, and $\nu 19a$.

Of the five hydrogen frequencies three belong to stretching vibrations and can be immediately assigned to the region 3050–55 cm^{-1}. The totally symmetric stretching frequency $\nu 2$ should be weak or missing in the infra-red; it is represented by the strong polarized Raman line at 3054 cm^{-1}. The antitranslational stretching $\nu 20a$ (as well as $\nu 20b$) is assigned to the strong, rather broad infra-red line at 3075 cm^{-1}; it seems likely that here as in monodeuterobenzene $\nu 20a$ and $\nu 20b$ form an unresolved doublet.

The position of $\nu 13$ is somewhat uncertain. The Raman line at 3054 cm^{-1} is surrounded by several satellites; these form a regular series corresponding to the combination tones $\nu 19b+\nu 8b$, $\nu 19b+\nu 8a$, $\nu 19a+\nu 8b$ (not observed but would be obscured by the strong line at 3054 cm^{-1}), and $\nu 19a+\nu 8a$, and it may be conjectured that these lines actually represent combination tones strengthened by resonance with $\nu 2$. As no valid assignments for $\nu 13$ and for $\nu 7b$ of class B_2 suggest themselves, both these frequencies are assigned with $\nu 2$ to 3054 cm^{-1}. These lines cannot be far distant, and the assignment proposed even if in error makes only a negligible difference in the calculation of thermodynamic quantities.

There remain in this class two hydrogen bending frequencies, $\nu 9a$ and $\nu 18a$, which are assigned to 1139 and 884 cm^{-1}, respectively. These two lines appear in the ultraviolet vibrational spectrum of Henri and Angenot[19]* and as they cannot be overtones must correspond to totally symmetric vibrations. Exact polarization data on the Raman line at 884 cm^{-1} are difficult, as the only intense observed line corresponding to this vibrational shift (22,050 cm^{-1} = Hg $e-888$) falls very near the strong highly polarized line $\nu 1$ (22,006 cm^{-1} = Hg $f-989$). The correctness of the location of $\nu 18a$ at 884 cm^{-1} therefore depends entirely on the correct analysis of the ultraviolet vibrational spectrum.

For $\nu 9a$ the ultraviolet line at 1159 cm^{-1} is correlated with the Raman and infra-red line at 1139 cm^{-1}, although this line appears but very slightly polarized if at all.

Class B_1

This class includes the vibrations in the plane of the molecule antisymmetric to the twofold rotational axis. The ring vibrations are $\nu 6b$, $\nu 8b$, $\nu 14$, and $\nu 19b$. The two hydrogen stretching frequencies $\nu 7b$ and $\nu 20b$ have already been assigned to 3054 cm^{-1} and 3075 cm^{-1}. There are three hydrogen bending frequencies corresponding to the four frequencies $\nu 3$, $\nu 9b$, $\nu 15$, and $\nu 18b$ in benzene; the assignment proposed is:

$$\nu 3 = 1210, \quad \nu 15 = 1139, \quad \nu 18b = 1037 \ cm^{-1}.$$

$\nu 3$ and $\nu 15$ lie in the general range 1100–1300 cm^{-1}.

$\nu 18b$ is assigned to 1037 cm^{-1} where there is an intense infra-red line which appears to be different from $\nu 12$ at 1028 cm^{-1}. A weak Raman line is also found at this point. $\nu 12$ is forbidden in the infra-red in benzene, and it seems unlikely that it would be so intense in pyridine vapor as the observed line at 1037 cm^{-1}.

$\nu 15$ is assigned to 1139 cm^{-1}. Two lines appear to be present in this region, of which one probably represents $\nu 9a$ and the other either $\nu 15$ or a combination tone.

Class B_2

This class contains those vibrations out of the plane of the molecule and antisymmetric to the twofold rotational axis. The ring vibrations are $\nu 4$ and $\nu 16b$. Three hydrogen vibrations are formed from $\nu 5$, $\nu 10b$, $\nu 11$, and $\nu 17b$ in benzene. $\nu 11$, the out-of-plane antitranslational bending is readily assigned to the strong infra-red line at 669 cm^{-1}, whose P, Q, and R branches are very similar to those of the corresponding line in benzene. $\nu 5$ is assigned to 941 cm^{-1}, somewhat lower than its position in benzene. $\nu 10$ in benzene is very intense in the infra-red spectrum of the liquid; the doublet $\nu 10a$, $\nu 10b$ in pyridine is assigned to 747 and 710 cm^{-1}, respectively, as both of these lines are very strong in the infra-red absorption of the liquid. In the vapor the line at 710 cm^{-1} appears as a shoulder on the strong infra-red line at 669 cm^{-1}. A weak line is also found at 744 cm^{-1}; this probably represents the overtone $2 \times \nu 16b = 748$ cm^{-1} as $\nu 10a$ is forbidden in the infra-red of pyridine.

Class A_2

This class contains the out-of-plane vibrations symmetrical to the twofold rotational axis. Frequencies are forbidden in the infra-red. The one ring vibration $\nu 16b$ falls at 374 cm^{-1}. Of the two hydrogen frequencies $\nu 10a$ has already been located at 747 cm^{-1}, and $\nu 17a$ is assigned to 1061 cm^{-1}, which is somewhat higher than the corresponding benzene frequency.

This assignment permits an explanation for the two infra-red lines at 1830 and 1991 cm^{-1} similar to that proposed by Pitzer and Scott for the corresponding benzene lines:

$$\nu 10a + \nu 17a = 747 + 1061 = 1808 \ cm^{-1},$$
$$\nu 5 + \nu 17a = 941 + 1061 = 2002 \ cm^{-1}.$$

Another assignment for 1808 cm^{-1}, however, seems more reasonable, as shown in Table I.

Other Lines Observed

Pyridine is notoriously difficult to purify, and commercial grades show a wide boiling range. The appearance of an unexplained group of lines in the pyridine spectrum suggests that the pyridine samples of the majority of investigators contained traces of α-picoline. The separation of this substance (b.p. 128°C) from pyridine (b.p. 115.5°C) requires distillation in a still of high

* Henri and Angenot themselves correlate the UV line at 857 cm^{-1} with the Raman line at 884 cm^{-1}.

TABLE V. Principal lines of liquid α-picoline.

Infra-red (Ref. 20)	Raman (Ref. 18)
	207 (4)
	547 (5)
	628 (3)
755 (10)	
	801 (6)
	813 (4)
993 (6)	996 (8)
1044 (7)	1048 (9)
1144 (4)	
	1235 (3)
	1374 (3)
1458 (6)	
	1568 (3)
1595 (8)	1592 (3)
	2922 (3)
2976 (5)	3041 (3)
	3066 (3)

efficiency, or careful chemical purification as employed by Turkevich and Stevenson.[23]

Table V gives the principal lines of α-picoline; it will be observed that in each case the lines are either present as weak unexplained lines in the pyridine spectrum or would be obscured by strong pyridine fundamentals. The suspected lines are missing in the vapor-phase infra-red spectrum of Turkevich and Stevenson.

The remaining lines of the pyridine spectrum are overtones and combinations, for which possible assignments are suggested in Table I.

THERMODYNAMIC PROPERTIES OF PYRIDINE

With the twenty-seven fundamental vibration frequencies of pyridine located in at least an approximate fashion, the thermal properties of pyridine vapors in the ideal-gas state may readily be calculated. Table VI summarizes the calculation of the entropy of the vapors at 25°C and one-atmosphere pressure; comparison with the experimentally measured value corrected to the ideal-gas state at one atmosphere shows good agreement. This shows that the frequencies proposed as fundamentals have at least an approximately correct distribution in the spectrum.

Table VII gives values of the free energy function $-(F^\circ - E_0^\circ)/T$, the heat content function $(H^\circ - E_0^\circ)$, and the heat capacity C_p° for pyridine vapors in the ideal-gas state at one-atmosphere pressure and temperatures up to 1000°K. These data are probably correct to within about five percent and should be sufficient for most engineering and thermodynamic calculations. Actual pyridine vapors probably differ appreciably from an ideal gas, so an appropriate equation of state should be used in calculations. These data permit the determination of equilibria involving pyridine with fair accuracy and the limiting factor is now the considerable uncertainty in the heat of combustion of pyridine.

In determining the thermal functions of Tables VI and VII the structure of pyridine was determined from the electron diffraction data of Schomaker and Pauling.[25] These authors calculated an average ring-bond distance of 1.385 $\pm$0.01 A.U., from which, assuming a carbon-carbon bond length of 1.39 A.U. as in benzene, they found the carbon-nitrogen bond length in pyridine to be 1.37$\pm$0.03 A.U.

To determine the bond angles it was assumed that the angles on each of the five carbon atoms were equal; these angles are then calculated to be 119.6° and the ring bond angle on the nitrogen

TABLE VI. Entropy of pyridine vapor in the ideal-gas state at one atmosphere and 25°C.

By statistical calculation:	
Translation and rotation	63.21 E. U./mole
Vibration	4.96
Total	68.17 E. U./mole
By experimental data:	
Entropy of liquid pyridine at 298.15°K	42.8$\pm$0.4 E. U./mole
Entropy of vaporization	33.0$\pm$0.3
Correction of actual gas at 20.7 mm* to ideal gas at 20.7 mm	0.0
Compression to 760 mm	−7.2
Total	68.6$\pm$0.7 E. U./mole

* Vapor pressure of pyridine at 25.0°C.

TABLE VII. Thermodynamic functions of pyridine vapor (for the ideal-gas state at one atmosphere).

T°K	$-(F^\circ - E_0^\circ)/T$ (Cal./degree)	$(H^\circ - E_0^\circ)$ Kcal./mole	C_p° Cal./degree
291.15	56.30	3.324	19.25
298.15	56.57	3.458	19.72
300	56.65	3.495	19.85
400	60.39	5.810	26.30
500	63.95	8.723	31.68
600	67.36	12.11	35.99
700	70.69	15.90	39.50
800	73.85	19.98	42.35
900	76.92	24.35	44.74
1000	79.87	28.93	46.76

atom 122.0°. It was further assumed that the carbon-hydrogen bonds bisect the angle supplementary to the ring bond angle. Using these assumptions the center of gravity of the molecule is found to lie on the C_2^z axis 1.36 A.U. above the nitrogen atom. This gives $\log ABC = -113.226$.

The 1941 atomic weights were used, and the tables of Wilson, as given by Aston for the new physical constants, for the harmonic oscillator contributions to the thermal functions.[30]

The experimental entropy of the vapor was based on the value of Parks, Todd, and Moore[31] for liquid pyridine. The vapor pressure and entropy of vaporization at 25°C were calculated from the vapor-pressure equation of van der Meulen and Mann.[32] Expansion of the vapor to infinite volume by the Berthelot equation of state and recompression to the vapor pressure at 25°C by the ideal gas law gave a negligible correction of −0.006 E.U.

ACKNOWLEDGMENT

The authors are indebted to Professor A. W. C. Menzies for selection of vapor-pressure data, and to Professor Henry Eyring for helpful discussions.

[30] Taylor and Glasstone, editors, *A Treatise on Physical Chemistry* (D. Van Nostrand Company, Inc., New York, 1942), Edition 3, Vol. I, Chap. IV.

[31] Parks, Todd, and Moore, J. Am. Chem. Soc. **58**, 398 (1936).

[32] van der Meulen and Mann, J. Am. Chem. Soc. **53**, 451–453 (1931).

The Molecular Structure and Thermodynamics of Propane

The Vibration Frequencies, Barrier to Internal Rotation, Entropy, and Heat Capacity

KENNETH S. PITZER[1]
Department of Chemistry, University of California, Berkeley, California

(Received April 17, 1944)

A substantially complete picture is proposed for the vibrational and torsional motions of the propane molecule. The vibrational assignment of Wu and Barker is extended and slightly revised so that definite values are assigned to all normal modes. It is believed that, with possibly one exception, all are correct within 2 percent. Comparison with the experimental entropy and heat capacity shows excellent agreement. The free energy, heat content, and heat capacity functions are then calculated over the range 180 to 1500°K. By obtaining the fundamental frequency of one torsional mode from a combination band in the infra-red spectrum, it was possible to evaluate the other from the entropy. The force constants calculable therefrom indicate that the apparent increase of potential barrier from ethane to propane arises from interaction of methyl group hydrogen atoms. For that mode in propane where these distances remain larger the torsional force constant is the same as that for ethane.

ALTHOUGH the existence of an appreciable barrier resisting rotation in propane is well known, it has not been possible previously to obtain various details of the forces within that molecule. In the present paper is presented a reasonably complete, but by no means absolutely proven, picture. It involves first a complete assignment of ordinary vibrational modes, second a calculation of the usual thermodynamic quantities based on a simplified rotational potential scheme, and finally a more detailed internal rotational analysis making use of both the infra-red spectrum and the entropy data.

VIBRATION FREQUENCIES

A number of partial or statistical assignments of vibration frequencies of propane[2–4] have been made, but in all cases some frequencies have been either missing or mere guesses. The most detailed assignment was that of Wu and Barker[4] based on their excellent infra-red absorption spectrum. By extending the Wu and Barker data with dynamical considerations and taking account of the work of Edgell and Glockler[5] and of Wagner[6] on the CH_2X_2 series of molecules, an assignment has been worked out which gives a definite value (within 2 percent) to all frequencies, accounts for the spectra, and agrees with the thermodynamic data for propane. This assignment is presented in Table I. It will be discussed according to types of motion below. Data for ethane,[7] methylene fluoride,[5,8] and methylene chloride[5,6] are given for comparison. While the CH_3 group is lighter than a fluorine atom, the greater distances, particularly to the hydrogen atoms, give it a greater effective moment of inertia for all vibrations of interest.

The data for these related molecules indicate that the carbon-hydrogen stretching modes are so close together in frequency that complete segregation is out of the question. The values given are certainly close to the correct ones for the same reason and a few are definitely identified from the spectra. Likewise the unsymmetrical bending or deformation motions within the methyl group all lie so close to 1460 cm^{-1} that separate identification is impossible. As in ethane, the two modes arising from symmetrical bending of the methyl group are close to 1375 cm^{-1}. The selection of 375 cm^{-1} for the skeletal bending

[1] Now on leave. Temporary address, Maryland Research Laboratories, Box 2706, Washington 13, D. C.
[2] G. B. Kistiakowsky and O. K. Rice, J. Chem. Phys. **8**, 610 (1940) (includes references to earlier work).
[3] K. S. Pitzer, Chem. Rev. **27**, 39 (1940).
[4] V. L. Wu and E. F. Barker, J. Chem. Phys. **9**, 487 (1941). G. B. Kistiakowsky and A. G. Nickel, *ibid.* **10**, 78 (1942) have offered apparently arbitrary values for those frequencies not included by Wu and Barker.
[5] G. Glockler and W. F. Edgell, private communications; see also G. Glockler, Rev. Mod. Phys. **15**, 111 (1943); W. F. Edgell, Thesis for Degree of Master of Science, State University of Iowa (1941).
[6] J. Wagner, Zeits. f. physik. Chemie **B45**, 69 (1939).
[7] F. Stitt, J. Chem. Phys. **7**, 297 (1939).
[8] G. Glockler and G. R. Leader, J. Chem. Phys. **7**, 382 (1939).

TABLE I. Vibration frequencies in cm^{-1}.

Molecule sym.	Sym. class	Allowed activity	C–C–C bending	C–C str.	CH_2, CH_2 wagging	CH_3 sym. bend.	CH_3 unsym. bending	CH_2 twisting	CH_2 sym. bending	CH_2 sym. str.	CH_3 unsym. str.	CH_2 str.
	A_{1g}	$R-$		993		1375				2925		
C_2H_6	A_{2u}	$-IR$				1380				2925		
(D_{3d})	E_u	$-IR$			827		1465				2980	
	E_g	$R-$			1170		1460				2960	
	A_1	R, IR	375	868	1155	1370	1468		1460	2914	2966	2960
C_3H_8	A_2	$R-$			940		1450	1278			(2970)	
(C_{2v})	B_1	R, IR		1053	922, 1338	1375	1470			2942	2968	
	B_2	R, IR			748, 1179		1450				2968	2980
	A_1	R, IR							1508			2963
CH_2F_2	A_2	$R-$						1294				
(C_{2v})	B_1	R, IR			1487							
	B_2	R, IR			1262							3030
	A_1	R, IR							1425			2985
CH_2Cl_2	A_2	$R-$						1149				
(C_{2v})	B_1	R, IR			1266							
	B_2	R, IR			896							3046

mode and 868 cm^{-1} and 1053 cm^{-1} for the skeletal stretching modes has been made by various authors already.

Of the remaining modes the symmetrical bending and the twisting of the CH_2 group are expected to be distinct enough in propane to be identified from the spectra of the CH_2X_2 series of molecules. From the pertinent values for CH_2F_2 and CH_2Cl_2 listed in Table I, the selection of the 1278 cm^{-1} Raman line is quite definite, particularly since it should be and is absent from the infra-red spectrum. The sym. bending motion is merely limited to the 1450 to 1500 cm^{-1} region already crowded with four methyl group motions. Probably the best indication of the value for this vibration is found in the spectra of cyclohexane and cyclopentane, neither of which contain any methyl groups. They show one or more lines in the 1440 to 1480 cm^{-1} range in both the infra-red and Raman spectra. The value 1460 may be adopted as probably correct within 2 percent.

Besides internal rotational modes which will be discussed later, there remain only the wagging motions of both CH_2 and CH_3 groups. The latter might be expected to have lower frequencies but serious interactions cannot be ruled out when the two wagging frequencies in ethane differ so greatly. The selections by Wu and Barker[4] of 922 cm^{-1} for class B_1, and 748 and 1179 for B_2 seem reasonably certain on the basis of band contours. The contour of the infra-red band near 1150 cm^{-1} is very much like that of the 867 cm^{-1} class A_1 band provided one takes the center at 1158 cm^{-1}. Therefore, with a Raman line reported at 1155 cm^{-1} assigned to class A_1, it seems best to classify that infra-red band as A_1 rather than B_1 as shown by Wu and Barker. Furthermore, the CH_2X_2 data suggest the range 1300 to 1400 cm^{-1} for the remaining mode of B_1 symmetry which is well above the 1150 cm^{-1} value and is far enough above the 922 cm^{-1} mode to make serious interaction unlikely. The 1338 cm^{-1} band has a sharper and more prominent Q branch than the 922 cm^{-1} B_1 class band which presumably led to the B_2 assignment by Wu and Barker. However, the 1338 cm^{-1} band has more prominent P and R branches than the class B_2 bands. This together with its similarity of P, Q, R spacing with the remaining B_1 bands and its location in the expected range lead to the assignment shown in Table I.

The final wagging motion is that of A_2 symmetry which is forbidden in the infra-red but is Raman active. In this motion one methyl wags up from the plane of the three carbons while the other goes down. In the 748 cm^{-1} class B_2 mode both methyls go up and down together. These modes are analogous to the 1170 and 827 cm^{-1} modes of ethane, respectively. The increased mass and moment of inertia of the propane skeleton and interaction with the higher CH_2

frequencies would be expected to decrease both of these frequencies and to decrease the higher one by a larger amount. The only unassigned Raman line in this region is that reported by Daure[9] at 940 cm^{-1} but not found by either Bhagavantam[10] or Kohlrausch and Köppl.[11] This value is adopted, but without any sense of certainty. The true value must be not far different in any case.

Before discussing the internal rotational motions the thermodynamic data on propane will be considered. This will be shown to support strongly the vibrational assignment of Table I.

It is interesting to note that where the CH_3 wagging frequencies are greatly reduced from ethane to propane, i.e., classes A_2 and B_2, the CH_2 frequencies are up near the CH_2F_2 values while otherwise the CH_2 frequencies are about midway between the CH_2F_2 and CH_2Cl_2 values. While this is no proof, it strongly suggests considerable interaction in the A_2 and B_2 classes and indicates that the "undisturbed" CH_3 frequencies would be higher and the CH_2 frequencies lower than the actual values in propane.

It is not yet possible either to show how well characteristic CH_2 and CH_3 frequencies will agree statistically with the actual frequencies or to select reliable sets of characteristic frequencies. Nevertheless the need for such information for calculation on more complex molecules is such that even highly tentative values are of interest. For the CH_3 group one may take the ethane frequencies (slightly rounded): 827, 1170, 1375, 1460 (2), 2950 (3). Then in propane the following sets of values are selected to be statistically equivalent to these and may be attributed to the two CH_3 groups: (748, 922), (1155, 1179), (1370, 1375), (1450, 1450, 1468, 1470), (2914, 2942, 2966, 2968, 2970). It will be noted that the 1179 frequency is actually more a CH_2 motion while the 940 cm^{-1} CH_3 frequency is not in this list. This is another manifestation of the interaction between CH_2 and CH_3 motions. We then arbitrarily select the remaining frequencies for the CH_2 group: 940, 1278, 1338, 1460, 2950 (2).

It will be shown in a paper to be published elsewhere that these frequency sets for the CH_2 and CH_3 groups actually give good agreement with the heat capacity data for the normal paraffins from butane to heptane.

TABLE II. The entropy of propane and the barrier to internal rotation. (Basis: hypothetical ideal gas at 1 atmos. pressure.)

	180.00°K	231.09°K	
Translation and rotation	54.57	56.56	cal./degree mole
Vibration	0.49	1.02	cal./degree mole
Total less internal rotation	55.06 ±0.05	57.58 ±0.05	cal./degree mole
Experimental	57.04 ±0.1	60.46 ±0.1	cal./degree mole
Internal rotation	1.98	2.88	cal./degree mole
Potential barrier to fit entropy (2 degrees of freedom)	3400 ±150	3390 ±150	cal./mole

THERMODYNAMIC PROPERTIES

In Table II calculations of the entropy of propane are compared with experimental values. The experimental data are taken from the work of Kemp and Egan[12] but are corrected to the value 273.16°K, for the ice point. The experimental entropy at 180°K was calculated using the vapor pressure data (together with the Berthelot equation for gas imperfection) to obtain an entropy of vaporization at that temperature.

The uncertainties shown in line three of Table II take account of the possibility that the 940 cm^{-1} Raman line is spurious and would allow for any reasonable assignment. In fact, the principal uncertainty is in the interatomic distances and angles. The following values were used: C−C, 1.54A; C−H, 1.09A; C−C−C angle 111° 30′; other angles tetrahedral.[13] On this basis the over-all moments of inertia are 2.88_5, 9.91_2, and 11.20_7 each $\times 10^{-39}$ g cm^2. The moment of inertia of a methyl group is 5.30×10^{-40} while the effective reduced moment is 4.51×10^{-40}. In these calculations R is taken as 1.98718 cal. per degree and hc/k as 1.43848 cm deg.

The barrier to internal rotation is calculated on the arbitrary assumption that each methyl group rotation is independent, i.e., no potential energy cross terms exist. This assumption will be discussed further below; however, it is not serious for the thermodynamic purposes of this

[9] P. Daure, Ann. de physique **12**, 375 (1929).
[10] S. Bhagavantam, Ind. J. Phys. **6**, 595 (1932).
[11] K. W. F. Kohlrausch and F. Köppl, Zeits. f. physik. Chemie **B26**, 209 (1934).
[12] J. D. Kemp and C. J. Egan, J. Am. Chem. Soc. **60**, 1521 (1938).
[13] L. Pauling and L. O. Brockway, J. Am. Chem. Soc. **59**, 1223 (1937).

TABLE III. The heat capacity of propane in cal. per degree mole.

Experimenter	T, °K	C_p^0 exp.	C_p^0 this research	Difference
Kistiakowsky,	148.2	11.69	11.56	−1.1%
Lacher and	157.8	12.04	11.88	−1.3
Ransom[a]	213.1	14.00	13.86	−1.0
(averaged	219.2	14.17	14.10	−0.5
values)	258.0	15.75	15.73	−0.1
Kistiakowsky and Rice[b]	272.38	16.19	16.38	+1.2
Kistiakowsky and Rice[b]	300.37	17.58	17.67	+0.5
Kistiakowsky and Rice[b]	334.05	19.25	19.30	+0.3
Kistiakowsky and Rice[b]	368.55	20.90	21.00	+0.5
Dailey and Felsing[c]	343.7	19.66	19.77	+0.5
Dailey and Felsing[c]	360.1	20.36	20.58	+1.1
Dailey and Felsing[c]	387.8	21.62	21.94	+1.4
Dailey and Felsing[c]	452.6	25.07	24.99	−0.3
Dailey and Felsing[c]	521.2	27.89	27.91	+0.1
Dailey and Felsing[c]	562.0	29.10	29.48	+1.3
Dailey and Felsing[c]	603.3	30.75	30.96	+0.7
Dailey and Felsing[c]	693.2	33.61	33.93	+1.0

[a] See reference 17.
[b] See reference 2.
[c] Dailey and Felsing, J. Am. Chem. Soc. **65**, 42 (1943).

section. The formulas and tables of Gwinn and the writer were used.[14] The potential barrier thus obtained, 3400 cal. per mole, happens to be identical with that originally estimated by the writer[15] in 1937 and is substantially the same as the values obtained by various workers since.[2, 12, 16, 17]

Table III compares the calculated heat capacity with the more recent and accurate experimental data for propane.

While the differences in Table III may slightly exceed the experimental error at certain points, one must consider the agreement excellent for

TABLE IV. Thermodynamic functions for propane. (Basis: hypothetical ideal gas at 1 atmos. pressure.)

T, °K	$\frac{(H_0^\circ - F_T^\circ)}{T}$ cal./deg.	$H_T^\circ - H_0^\circ$ kcal.	C_p° cal./deg.
180.00	47.38	1.745_5	12.64
231.09	49.90	2.440	14.57
298.16	52.73	3.512	17.57
400	56.48	5.558	22.54
500	59.81	8.040	27.04
600	62.93	10.92_5	30.84
800	68.74	17.77	37.08
1000	74.10	25.67	41.83
1500	85.85	48.64	49.26

such a complex molecule. It shows that the vibrational assignment must be substantially correct. Either the doubtful frequency (here taken as 940 cm^{-1}) or the approximate treatment of internal rotation may be in error enough to account for the 0.1 cal. per degree differences appearing in Table III.

The thermodynamic functions, $(H_0^\circ - F_T^\circ)/T$, $H_T^\circ - H_0^\circ$, and C_p are given in Table IV for a series of temperatures. The entropy is easily calculated from the equation:

$$S = (H_0^\circ - F_T^\circ)/T + (H_T^\circ - H_0^\circ)/T.$$

The heat of formation[18] of propane gas at 298.16°K is $\Delta H^\circ = -24.822 \pm 0.142$ kcal. The standard free energy of formation[19] is therefore $\Delta F^\circ_{298.16} = -5.597$ kcal. and the heat of formation at the absolute zero is $\Delta H_0^\circ = -19.487$ kcal.

INTERNAL ROTATION

Although a value of the potential barrier to internal rotation was obtained on the basis of certain assumptions in the preceding section, certain other information can be brought to bear on this problem. The data of Wu and Barker[4] show a moderately weak infra-red band at 720 cm^{-1} whose band contour rather definitely indicates the B_2 symmetry class. Since there is no reasonable explanation of this band as a fundamental, overtone, or sum-combination, it is presumed to be a difference-combination band. Then its intensity is reasonable only if the lower frequency is very low, either an internal rotational (torsional vibration) level or the 375 cm^{-1} state. The latter would call for a B_2 band at 1095 cm^{-1} and is thus excluded. Table V lists the various remaining possibilities.

TABLE V. Possible values of torsional vibrational level to explain 720 cm^{-1} band.

Sym. class	Frequency	Difference—combination
A_2	202 cm^{-1}	$922 - 202 = 720$ cm^{-1}
A_2	333	$1053 - 333 = 720$
B_2	148	$868 - 148 = 720$
B_2	435	$1155 - 435 = 720$

[14] K. S. Pitzer and W. D. Gwinn, J. Chem. Phys. **10**, 428 (1942).
[15] K. S. Pitzer, J. Chem. Phys. **5**, 473 (1937).
[16] K. S. Pitzer, Chem. Rev. **27**, 39 (1940).
[17] G. B. Kistiakowsky, J. R. Lacher, and W. W. Ransom, J. Chem. Phys. **8**, 970 (1940).
[18] E. J. Prosen and F. D. Rossini, to be published in J. Research Nat. Bur. Stand. (1944).
[19] These calculations involve the thermodynamic functions for graphite from Clayton and Giauque [J. Am. Chem. Soc. **54**, 2610 (1932)] and for hydrogen from Giauque [*ibid.* **52**, 4816 (1930)] revised to the present physical constants of Woolley, Brickwedde, and Scott (to be published).

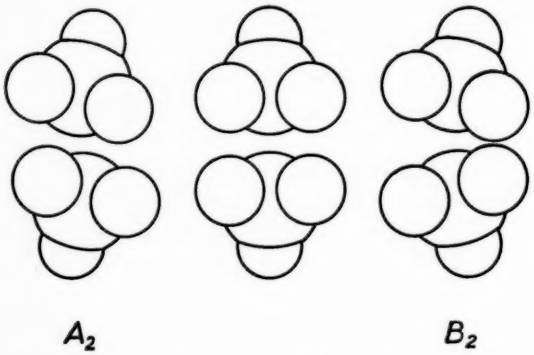

FIG. 1. Diagram showing small distortions of the molecule in the torsional modes of symmetry classes A_2 and B_2, respectively. Only the methyl groups are shown.

In order to select among the possibilities shown in Table V, the mean frequency (of the two modes) necessary to explain the entropy contribution* of 1.98 cal. per degree at 180°K is calculated to be 238 cm^{-1}. Since no very large separation of the two energy levels is expected, the first line in Table V seems most reasonable. The entropy contribution from the 202 cm^{-1} mode is 1.24 cal. per degree at 180°K, leaving 0.74 for the class B_2 mode. This gives a frequency value of 283 cm^{-1} for the B_2 torsional mode.

Having determined both frequencies one can calculate the potential function near the equilibrium position by the usual harmonic oscillator methods. The equations have been presented by Dr. W. D. Gwinn and the writer[14] in a form appropriate to the present problem. In the following analysis reference will be made to this paper as (P. and G.).

The potential energy for the torsional motions of very small amplitude is written, following Eq. (33) (P. and G.),

$$2V=b_{11}(\varphi_1^2+\varphi_2^2)+2b_{12}\varphi_1\varphi_2,$$

where φ_1 and φ_2 are the angles of motion of the respective methyl groups from their equilibrium positions. The inertial quantities needed are $A=5.30\times10^{-40}$ the moment of inertia of a methyl group and

$$\Lambda_{11}=\Lambda_{22}=A^2\sum_{i=1}^{3}\lambda_i^2/I_i$$

and

$$\Lambda_{12}=A^2\sum_{i=1}^{3}\lambda_{1i}\lambda_{2i}/I_i,$$

in which the I_i's are over-all rotation moments of inertia and the λ_i's are direction cosines between the methyl axes and the principal axes of the molecule. In these terms $\Lambda_{11}=0.75_5\times10^{-40}$ and $\Lambda_{12}=-0.57_6\times10^{-40}$ g cm^2.

The determinantal equation [(36), P. and G.] can be factored by symmetry into the following:

$$b_{11}+b_{12}-(A-\Lambda_{11}+\Lambda_{12})4\pi^2\nu^2=0$$
Class B_2, $\nu c=283$ cm^{-1},

$$b_{11}-b_{12}-(A-\Lambda_{11}-\Lambda_{12})4\pi^2\nu^2=0$$
Class A_2, $\nu c=202$ cm^{-1}.

One then finds $b_{11}+b_{12}=1.12\times10^{-12}$ erg per radian^2 and $b_{11}-b_{12}=0.74\times10^{12}$ erg per radian^2 or $b_{11}=0.93\times10^{-12}$ and $b_{12}=0.19\times10^{-12}$.

The class A_2 motion would be expected to have the lower force constant since it starts to stagger the hydrogen atoms rather than pressing them close together. This is shown in Fig. 1. It is interesting to compare the torsional force constant from ethane, 0.71×10^{-12}, with the value of $b_{11}-b_{12}=0.74\times10^{-12}$. The difference is hardly significant considering the approximation and many steps involved. Rather, the conclusion may be drawn that the potential function for the A_2 class torsional motion in propane is substantially the same as that for ethane. The increased force for the B_2 class motion may be attributed to interference between methyl group hydrogen atoms.

These results lead to the presumption (not an absolute deduction) that the apparent increase in potential through the series ethane, propane, iso-butane, and neo-pentane is due to interferences of the methyl group hydrogen atoms rather than increase of the potential barrier attributable to a given carbon-carbon bond on substitution of methyl groups at one end. This tentatively answers a question which was studied but not answered in a previous publication.[20] It will be interesting, when circumstances allow the time, to investigate a complete internal rotational potential function consistent with these force constants and other boundary conditions.

* At this low a temperature the difference between a harmonic (torsional) osillator and the restricted rotator is small and will be neglected.

[20] K. S. Pitzer, J. Chem. Phys. **10**, 605 (1942).

THE JOURNAL OF CHEMICAL PHYSICS VOLUME 12, NUMBER 7 JULY, 1944

The Crystal Structure of Ni_4Mo

DAVID HARKER
Research Laboratory, General Electric Company, Schenectady, New York

(Received April 24, 1944)

A nickel-molybdenum alloy containing about 20 atom percent of molybdenum exists above 900°C as a cubic close-packed structure. If this alloy is quenched and then held at temperatures below 840°C, an ordering reaction occurs which results in a slight tetragonal distortion of the cubic structure. This ordered structure requires for its description a tetragonal cell with 2.5 times the volume of the distorted face-centered cubic cell. The completely ordered structure can be described analytically as follows: space group: C_{4h}^5-I4/m; dimensions of unit cell: $a_0=5.720$A, $c_0=3.564$A, $c/a=0.6231$; atomic positions: 2 Mo in 2(*a*), 8 Ni in 8(*h*), $x=0.200$. $y=0.400$.

THE nickel-molybdenum alloys have been studied rather extensively and two complete phase rule diagrams have been published. Grube and Schlecht[1] report an ordering reaction in the nickel rich solid solution; Ellinger[2] interprets the behavior of the same alloys as being due to the precipitation of a new phase.

In an attempt to decide this question, some x-ray diffraction patterns were prepared of a 27.3 weight percent molybdenum in nickel alloy. This composition is 18.7 atom percent molybdenum and can be written $Ni_{4.065}Mo_{0.935}$, which is close to Ni_4Mo.

The alloy was vacuum cast from electrolytic nickel and pure molybdenum, swaged hot to 0.040-inch rod from the 1.4-inch cast bar, with eight-hour treatments at 1200°C at the 1-inch, 0.5-inch, 0.25-inch, and 0.1-inch stages of the swaging. The specimens for x-ray work were etched to 0.027-inch diameter after the last previous heat treatment. The diffraction patterns were obtained in a cylindrical camera, using copper *K* radiation filtered through 0.001-inch nickel foil.

The alloy gave a powder pattern characteristic of a cubic close-packed solid solution when quenched from 1200°C; but on subsequently holding the alloy at temperatures between 700°C and 825°C, i.e., "aging," the lines on the patterns gradually changed. At low holding temperatures, or short holding times, the change was evident only in a blurring of all the powder lines, except (111) and (222); at higher temperatures and longer holding times the blurred lines split into two or three components; and when the alloy had been heated at 800°C for six hours new, weak lines appeared.

This sequence of x-ray diffraction effects is very reminiscent of that found by the author[3] to occur during the low temperature aging of gold-copper alloys near the composition AuCu, and suggests that a similar ordering reaction is taking place.

The quenched Ni_4Mo alloys have a face-centered cubic unit cell containing four atoms and whose edge is $a_0=3.612$A. After being held at 800°C for some time, the cell changes to tetragonal, with $a_0=3.618$A and $c_0=3.567$A, $c/a=0.986$, if the new, faint lines are not taken into account. However, it was found impossible to index the new lines on the basis of this cell.

If **a**, **b**, and **c** are the vectors defining the tetragonal unit cell just described, then a new tetragonal cell with the defining vectors

$$\mathbf{a}'=\tfrac{1}{2}(3\mathbf{a}-\mathbf{b}),$$
$$\mathbf{b}'=\tfrac{1}{2}(\mathbf{a}+3\mathbf{b}),$$
$$\mathbf{c}'=\mathbf{c}$$

accounts for all the lines in the powder pattern of the aged specimens. The relation between the two cells is shown in Fig. 1. Since $a_0'=(5/2)^{\frac{1}{2}}a_0$ and $c_0'=c_0$, the volume of this new cell is 2.5 times the volume of the small tetragonal cell and it therefore contains ten atoms: 8 Ni and 2 Mo, in round numbers. On assigning indices to the lines on the basis of the new cell, it was found that $h+k+l$ was even in all cases and the cell is, consequently, body centered. No other system-

[1] G. Grube and H. Schlecht, Zeits. f. Elektrochemie **44**, 413 (1938).
[2] F. H. Ellinger, Trans. Am. Soc. Metals **30**, 607 (1942).
[3] D. Harker, Trans. Am. Soc. Metals **32**, 210 (1944).

atic absences were found. The space group is, therefore, one of these:

$$S_4^2,\quad C_4^5,\quad C_{4h}^5,\quad D_{2d}^9,\quad D_{2d}^{11},\quad C_{4v}^9,\quad D_4^9,\quad D_{4h}^{17}.$$

All but the first three of these can be eliminated at once, since all structures based on them demand absurdly small interatomic distances. The three remaining space groups provide the following structures:

A: $S_4^2-I\,\bar{4}$: 2 Mo in 2 (a)
8 Ni in 8 (g)
parameters: x', y', z'

B: $C_4^5-I\,4$: 2 Mo in 2 (a)
8 Ni in 8 (c)
parameters: x', y', z' ($z_{\mathrm{Mo}}=0$)

C: $C_{4h}^5-I\,4/m$: 2 Mo in 2 (a)
8 Ni in 8 (h)
parameters: x', y'. ($z'=0$).

The notation is that used in the *Internationale Tabellen zur Bestimmung von Kristallstrukturen*.[4] These structures differ only in the z' coordinates of the atoms. All have the same projection on the x', y' plane.

The physical process by which the structure is formed suggests that the atoms are nearly in the mutual relationship found in cubic close-packing. In the cell defined by the vectors **a**, **b**, **c**, the atomic coordinates are $x, y, z=0,0,0$; $0,\frac{1}{2},\frac{1}{2}$; $\frac{1}{2},0,\frac{1}{2}$; $\frac{1}{2},\frac{1}{2},0$; and positions derived from these by lattice translations. If x', y', z' are the atomic coordinates in the cell defined by **a'**, **b'**, **c'**, then

$$x'=(1/5)(3x-y),$$
$$y'=(1/5)(x+3y),$$
$$z'=z.$$

If the atomic positions change but little during the transformation, the primed coordinates must be nearly those provided by structures A, B, or C with $x'=0.2$, $y'=0.4$, $z'=0$.

It was assumed that $z=0$, as a first approximation, thus limiting the structure to C, and intensities were calculated from the formula

$$I_{hkl}=\text{const.}\times\frac{1+\cos^2 2\theta}{\sin^2\theta\cos\theta}p_{hkl}F_{hkl}^2A_\theta,$$

[4] *Internationale Tabellen zur Bestimmung von Kristallstrukturen* (Gebrüder Borntraeger, Berlin, 1935).

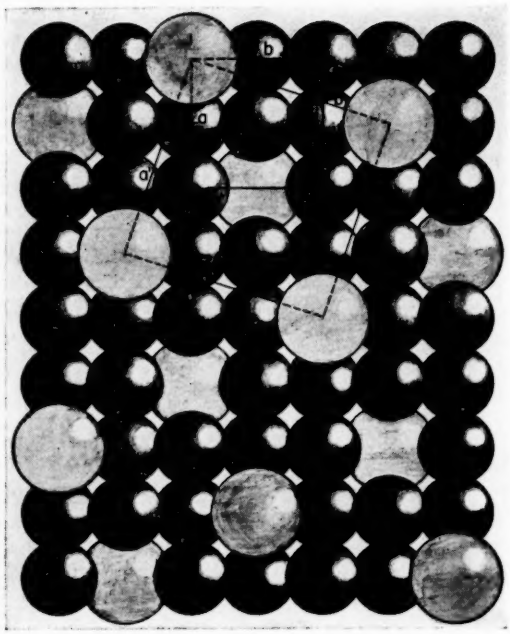

FIG. 1. The Ni_4Mo structure, viewed along [001]. The large lightly shaded atoms are Mo, the small heavily shaded atoms are Ni.

where θ is the glancing angle, p_{hkl} is the number of planes in the form $\{hkl\}$, A_θ is the correction for absorption in the powder rod, and F_{hkl} is given by

$$F_{hkl}=f_{\mathrm{Mo}}+2f_{\mathrm{Ni}}[\cos 2\pi(hx'+ky') + \cos 2\pi(hy'-kx')],$$

where f_{Mo} and f_{Ni} are the scattering factors of molybdenum and nickel, respectively. Intensities of all lines of the types $(h0l)$ and (hhl) were calculated for the parameter ranges $0.18<x'<0.22$, $0.38<y'<0.42$. The only satisfactory values were in the immediate neighborhood of $x'=0.200$ and $y'=0.400$. The intensities of some of the lines change very rapidly with the atomic positions, so that these parameters cannot vary by as much as 0.005 without completely destroying the agreement between the observed and calculated values. Inasmuch as the agreement is satisfactory, no attempt was made to vary the z' parameter from its value of 0.000.

The intensities of all lines appearing in the diffraction pattern of the completely ordered specimen were then calculated. The results of this calculation appear in Table I, where the observed intensities and the positions of the lines

are also listed. Since the observed and calculated intensities are in satisfactory agreement, and no data have been found which contradict the assumed structure, it can be taken as correct.

DISCUSSION OF THE STRUCTURE

The atomic arrangement in Ni_4Mo is very close to cubic close-packing: Each atom has twelve neighbors at very nearly equal distances. It is only when the kinds of atoms are differentiated that the structure can be characterized.

The twelve nearest neighbors of a molybdenum atom are all nickel atoms, while the neighbors of a nickel atom are nine nickel and three molybdenum atoms. All the nickel atoms are crystallographically equivalent, as are all the molybdenum atoms.

Oddly enough, the nickel-nickel and nickel-molybdenum distances are equal to one another. A nickel atom has three Ni and one Mo neighbor at 2.554A and six Ni and two Mo neighbors at 2.538A; the first of these sets of distances is parallel to the tetragonal base plane, the second is not. The Ni-Ni distance in pure nickel is 2.487A, so that it might have been expected that the Ni-Ni distance in Ni_4Mo would be smaller than it is; however, all structures based on a smaller Ni-Ni distance are rigorously excluded by the intensity data. Agreement between observed and calculated intensities is completely impossible of attainment for structures based on Ni-Ni distances differing from 2.538A by as much as 0.010A.

The Ni_4Mo structure is the fifth superstructure of the face-centered cubic lattice so far found; the other four are the AuCu, the $AuCu_3$, and the two CuPt structures. Like these, it contains only one crystallographic kind of each atomic species; all the nickel atoms have physically identical surroundings, and so have all the molybdenum atoms.

An interesting feature of the Ni_4Mo structure is the number of orientations it can have with respect to the face-centered cubic solid solution from which it forms. In the first place, the c axis of the tetragonal cell can be in any of the three original cube edge directions. Secondly, the tetragonal a axis can be either at a small positive or negative angle to an original cube edge direction. Finally, the tetragonal structure can have its origin at any of five positions—marked 1, 2, 3, 4, and 5 in Fig. 1. Thus, there are $3\times2\times5=30$ ways in which the Ni_4Mo structure can be situated in a region that was originally a single crystal of face-centered cubic solid solution. Inasmuch as the ordering reaction doubtless initiates at many points in each solid solution crystal, and at each point can choose any of thirty ways to grow (six orientations, five starting points), a crystal of the solid solution becomes a very complicated array of Ni_4Mo crystals as the ordering reaction proceeds.

Local distortions of the original cubic structure, such as would be produced by this complex arrangement of tetragonal regions, should make slip more difficult. The increase in hardness which accompanies the ordering reaction in this alloy can be explained on this basis. The author[3] has treated a similar situation in the gold-copper alloys in considerable detail.

TABLE I. Observed and calculated intensities for an x-ray powder diffraction pattern of Ni_4Mo using Cu $K\alpha$ radiation.

hkl	2θ obs.	*I* calc.	*I* obs.	*hkl*	2θ obs.	*I* calc.	*I* obs.
110	22.6	0.13	v wk	611	115.9	0.18	v wk
101	30.1	0.18	m wk	$620\alpha_1$	116.8	2.30	m
200	31.9	0.08	wk	$620\alpha_2$	117.2	1.35	m wk
211	44.1	10.7	v st	413			
220	45.4	0.06	wk	$004\alpha_1$	119.7	1.30	m
310	50.9	4.34	st	$004\alpha_2$	120.3	0.65	m wk
002	51.8	2.06	st	442	122.2	0.11	wk
301	55.0	0.07	wk	114	124.5	0.11	wk
112	57.0	0.08	m wk	541	125.2	0.22	wk
202	61.8	0.07	m wk	532	127.3	0.25	wk
321	64.8	0.15	m wk	204	129.5	0.14	wk
400	66.6	0.04	v wk	602	133.0	0.15	wk
330	69.9	0.03	v wk	$631\alpha_1$	136.1	7.69	m st
222	70.6	0.06	wk	$631\alpha_2$	136.9	3.92	m
411	73.5	0.13	m wk	$503\alpha_1$	138.1	16.2	st
420	74.5	2.65	m st	$433\alpha_1$			
312	75.2	5.16	st	$503\alpha_2$	138.8	8.13	m st
103	83.1	0.06	wk	$433\alpha_2$			
510	87.1	0.06	v wk	$224\alpha_1$	141.4	0.13	wk
402	87.9	0.06	v wk	$224\alpha_2$	142.4	0.06	v wk
501	90.3	9.60	st	$710\alpha_1$	143.9	9.80	m
431				$550\alpha_1$			
213	91.6	4.91	st	$710\alpha_2$	144.9	14.95	m st
332				$550\alpha_2$			
422	96.0	5.09	m st	$622\alpha_1$			
521	98.7	0.15	wk	$622\alpha_2$	145.9	5.20	m wk
440				$314\alpha_1$	148.7	12.0	m st
303	99.6	0.06	wk	$314\alpha_2$	149.9	6.08	m
530	103.9	0.07	v wk	$523\alpha_1$	152.5	0.40	wk
600	108.6	0.33	m wk	$523\alpha_2$	153.7	0.20	v wk
323							
512							

v st = very strong; st = strong; m st = medium strong; m = medium; m wk = medium weak; wk = weak; v wk = very weak.

(a) The intensities of (*hkl*) and (*khl*) are, in general, not the same, but, since the two planes reflect at the same angle, their intensities were added to give the calculated intensity listed in the table opposite the symbol (*hkl*).

(b) The lines for which $2h+k$ or $h+2k$ is a multiple of 5 can be indexed on the basis of the small cell in Fig. 1. They are the lines into which the lines of the face-centered cubic solid solution split during the ordering reaction. These lines were sharper and stronger than the others, so that their α_1, α_2 doublets could be resolved at smaller values of 2θ.

The Dissociation of Ammonium Chloride*

C. C. STEPHENSON
Research Laboratory of Physical Chemistry, Massachusetts Institute of Technology, Cambridge, Massachusetts

(Received April 26, 1944)

Two values for the standard free energy of dissociation of ammonium chloride into ammonia and hydrogen chloride, calculated by two independent paths, are 21,860 cal. and 21,780 cal. at 298.1°K. The good agreement serves as additional evidence for the complete dissociation of ammonium chloride in the vapor phase. The corresponding values calculated for ΔH at 298.1 are 42,160 and 42,260 cal. Two independent values for the standard entropy of the aqueous ammonium ion at 298.1°K derived from these data are 26.5 and 27.1 cal. mole^{-1} deg.$^{-1}$.

THE vapor densities and dissociation pressures of ammonium chloride have been the subject of a number of investigations;[1–5] the observed dissociation pressures are in good agreement, but the earlier vapor densities indicated partial dissociation of the vapor to NH_3 and HCl whereas the later measurements show that the vapor is completely dissociated. An independent approach to the equilibrium $NH_4Cl(s)=NH_3(g)+HCl(g)$ is possible from available thermal studies.

The entropies at 298.1°K of NH_4Cl,[6] NH_3,[7] and HCl[8] are 22.6, 46.03, and 44.66 units, from which $\Delta S^\circ_{298.1}=68.1$ for the above reaction. Thomsen[9] gives 41,900 cal. for ΔH, and Berthelot[10] finds 42,600 cal.

The heat capacity of NH_4Cl has been measured from room temperature to 525°K by H. Klinkhardt.[11] At 457.6°K a transition occurs for which $\Delta H=970$.[12] The thermodynamic properties of NH_3 and HCl at higher temperatures are given by Stephenson and McMahon and by Giauque and Overstreet. From these data and the equations $\Delta F^\circ=-RT\ln p_2/4=\Delta H^\circ-T\Delta S^\circ$, $\Delta H^\circ=\int\Delta C_P dT$, and $\Delta S^\circ=\int\Delta C_P d\ln T$, the dissociation pressures may be calculated. Within the limits of error of the experimental data the calculated pressures agree with the measured pressures, and confirm the more recent observations that the vapor is completely dissociated.

Since the greatest uncertainty lies in the value of ΔH°, it is profitable to reverse the calculations and obtain a more reliable value of ΔH° from the dissociation pressures and heat capacities. The constancy of the ΔH° values calculated from the dissociation pressures is a stringent test of the assumption of complete dissociation and of the dissociation pressure data. From the data of Rodebush and Michalek, $\Delta H^\circ_{298.1}=42{,}100\pm40$; from the data of Smits and Lange, $\Delta H^\circ_{298.1}=42{,}130\pm40$; from the data of Smith and Lombard, $\Delta H^\circ_{298.1}=42{,}090\pm40$; and from the data of Braune and Knoke, $\Delta H^\circ_{298.1}=42{,}190\pm10$. Only the data of Smith and Lombard show a trend in the calculated ΔH° values, and this trend is probably caused by an incorrect temperature scale. The data of Braune and Knoke are the most consistent. The value $\Delta H^\circ_{298.1}=42{,}160$ cal. is adopted, from which $\Delta F^\circ_{298.1}=21{,}860$.

* Contribution No. 508 from the Research Laboratory of Physical Chemistry, Massachusetts Institute of Technology.

[1] A. Smith and R. P. Calvert, J. Am. Chem. Soc. **36**, 1363 (1914).
[2] A. Smith and R. H. Lombard, J. Am. Chem. Soc. **37**, 38 (1915).
[3] H. Braune and S. Knoke, Zeits. f. physik. Chemie **135** 49 (1928).
[4] W. H. Rodebush and J. C. Michalek, J. Am. Chem. Soc **51**, 748 (1929).
[5] A. Smits and W. de Lange, J. Chem. Soc., p. 2947 (1928).
[6] W. T. Ziegler and C. E. Messer, J. Am. Chem. Soc. **63**, 2694 (1941).
[7] C. C. Stephenson and H. O. McMahon, J. Am. Chem. Soc. **61**, 437 (1939).
[8] W. F. Giauque and R. Overstreet, J. Am. Chem. Soc. **54**, 1731 (1932).
[9] J. Thomsen, *Thermochemische Untersuchungen* (Leipzig, 1882), Vol. 2, p. 406.
[10] M. Berthelot, *Thermochimie* (Paris, 1897), Vol. 2, p. 221.
[11] H. Klinkhardt, Ann. d. Physik [4] **84**, 188 (1924).
[12] P. W. Bridgman, Proc. Am. Acad. Arts Sci. **52**, 138 (1916/1917).

These results may be represented to a satisfactory degree of approximation by taking $\Delta C_p = -7.7$ from 298.1 to 457.6°K, and $\Delta C_p = -5.5$ above the transition temperature. Then $\Delta H^\circ = 44{,}460 - 7.7T$ from 298.1 to 457.6°K and $\Delta H^\circ = 42{,}490 - 5.5T$ above 457.6°K. Then $\Delta F^\circ = 44{,}460 + 17.7T \log T - 119.7T$ below 457.6°K, and $\Delta F^\circ = 42{,}490 + 12.7T \log T - 101.9T$ above the transition temperature. The dissociation pressures above 457.6°K are then given by $\log p_{\text{atmos}} = -4644/T - 1.38 \log T + 11.43$.

The free energy and heat of formation of NH_4Cl from NH_3 and HCl may be obtained by another path. The solubility of NH_4Cl at 25°C is $7.38M$, and the activity coefficient, from vapor pressures of aqueous solutions, of the saturated solution is 0.611.[13] The free energy of solution is then $\Delta F^\circ = -RT \ln (0.611 \times 7.38)^2 = -1780$. A less reliable value for the free energy of solution, $\Delta F^\circ = -1700 \pm 150$, may be derived from cell measurements by Brönsted.[14] The heat of solution in 120 moles of water at 25°C is 3730 cal.,[15] and the heat of dilution[16] is −126 cal.; hence, $\Delta H^\circ = 3600$. These values are combined with the following reactions at 298.1°K:

	ΔF°	ΔH°
$NH_3(g) + H_2O(1) = NH_4OH(aq)$	− 2,390[17]	− 8,285[18]
$NH_4OH(aq) = NH_4^+ + OH^-$	6,520[19]	865[20]
$H^+ + OH^- = H_2O(1)$	−19,093[21]	−13,358[20]
$HCl(g) = H^+ + Cl^-$	− 8,598[22]	−17,880[23]
$NH_4^+ + Cl^- = NH_4Cl(s)$	+ 1,780	− 3,600
$NH_3(g) + HCl(g) = NH_4Cl(s)$	−21,780	−42,260.

The agreement between the two independent values of ΔF° and ΔH° is very good. Using the averages of these two values and the standard heat and free energies for NH_3[7] and HCl,[23] the corresponding values $\Delta F^\circ = -48{,}460$ and $\Delta H^\circ = -75{,}200$ are obtained for NH_4Cl.

Two independent values for the entropy of the ammonium ion may be derived from these reactions. From the first three equations and the entropy of $NH_3(g)$, $S^\circ_{NH_4^+} = 26.5$; from the last two equations and the entropies of $HCl(g)$ and $NH_4Cl(s)$, $S^\circ_{NH_4^+} = 27.1$. A third value, 26.2, may be derived from the entropy of $NH_4H_2PO_4$. The average, 26.6 ± 0.5 cal. deg.$^{-1}$ mole^{-1}, is recommended for the entropy of the ammonium ion.

[13] J. N. Pearce and G. G. Pumplin, J. Am. Chem. Soc. **59**, 1219 (1937).
[14] J. N. Brönsted, Zeits. f. physik. Chemie **77**, 129 (1911).
[15] P. Mondain-Monvel, Ann. de chimie **10**, 3, 72 (1925).
[15] H. Streeck, Zeits. f. physik. Chemie **169**, 111 (1934).
[17] *International Critical Tables* (McGraw-Hill Book Company, Inc., New York, 1923), Vol. VII, p. 240.
[18] Reference 17, Vol. V, p. 213.
[19] D. H. Everett and W. F. K. Wynne-Jones, Proc. Roy. Soc. London **A169**, 190 (1938).
[20] K. W. Pitzer, J. Am. Chem. Soc. **59**, 2368 (1937).
[21] H. S. Harned and G. E. Mannweiler, J. Am. Chem. Soc. **57**, 1873 (1935).
[22] M. Randall and L. E. Young, J. Am. Chem. Soc. **50**, 989 (1928).
[23] F. D. Rossini, Bur. Stand. J. Research **9**, 679 (1932).

Erratum: Raman Spectra of Acetylenes. VII. Symmetrical-Top Acetylenes

[J. Chem. Phys. 11, 450 (1943)]

FORREST F. CLEVELAND, *Department of Physics,*

AND

M. J. MURRAY, *Department of Chemistry,*
Illinois Institute of Technology, Chicago, Illinois

HERZBERG has pointed out[1] that difference bands cannot be involved in Fermi resonance with a fundamental of nearly the same frequency, as was indicated in the paper referred to above, because the energy states of the upper levels in the two cases are too widely different. While the energy of the two absorbed quanta, for example, $hc(2200\ \text{cm}^{-1})$ and $hc(2900-700\ \text{cm}^{-1})$, *are* nearly equal, these are, of course, not the energies involved in Fermi resonance, which must be actual energy states of the molecule.

Consequently, the assignments in Table I of the paper should be revised insofar as the four difference bands are concerned. The (2892 – 691) and (2900 – 692) difference bands for 1-iodo-1-propyne and 1-bromo-1-propyne, respectively, are not needed to explain the appearance of the two weak lines near the strong triple bond line at 2200 cm^{-1} and should therefore be deleted from the table.

This leaves the difference bands (1438 – 343) and (1443 – 343) for the iodo and bromo compounds, respectively. These difference bands may actually appear and account for the very weak lines observed at 1150 and 1154 cm^{-1}, since the Boltzmann factor would be relatively large for the 343-cm^{-1} frequency. However, if this is the case, the corresponding summation bands (1438+343) and (1443+343), being undiminished by a Boltzmann factor, should appear with greater intensities than those observed for the 1150 and 1154 lines, and they were not observed. A more probable explanation of the 1150 and 1154 lines is that they correspond to the summation bands (410+691) and (464+692) for the iodo and bromo compounds, respectively.

Fermi resonance would not be permitted for the difference bands for the reason given in the first paragraph nor for the summation bands just mentioned since they are of type A_1 whereas the fundamental near 1025 is of type E. Hence the frequencies used in the heat capacity calculations should be 1021 and 1026 for the two compounds, rather than 1030 and 1035 cm^{-1} as given in Table IV of the paper. This would increase each of the calculated heat capacities listed in Table V of the paper by 0.02 calorie/(mole-degree).

[1] G. Herzberg, private communication.

Letters to the Editor

PROMPT publication of brief reports of important discoveries in physics may be secured by addressing them to this department. The closing date for this department is the third of the month. Because of the late closing date for the section no proof can be shown to authors. The Board of Editors does not hold itself responsible for the opinions expressed by the correspondents. Communications should not in general exceed 600 words in length.

Surface Tension and van der Waals' Equation

F. C. AULUCK AND R. N. RAI
University of Delhi, Delhi, India
May 29, 1944

IN recent years the theory of the liquid state has attracted considerable attention and several models have been proposed with the object of deriving the essential properties of liquids by applying the methods of statistical mechanics. The model which is of interest to us here is that of Fürth,[1] in which the liquid is assumed to be a continuum permeated with holes. The number of holes is taken to be equal to the number of molecules in the liquid. This picture of a liquid is just the reverse of the picture of a gas in the kinetic theory, for in the former case almost empty holes are supposed to move in a continuous material medium whereas in the latter case material particles move in empty space. The holes contain vapor at the vapor pressure corresponding to the temperature of the liquid.

The size of a hole in Fürth's treatment is not treated as fixed, but the hole can expand and contract and the probability distribution of the size is determined by an application of Boltzmann's law in the usual manner.

Fürth's theory easily leads to an expression for the intrinsic pressure p_0 in the liquid[2]

$$p_0 = 1.3[\sigma^4/(kT)^4], \tag{1}$$

where k is the Boltzmann constant, T the absolute temperature, and σ the surface tension at that temperature.

TABLE I.

Substance	p_0 in atmos.	a_2*	Substance	p_0 in atmos.	a_2
K	50×10^3	31×10^{-2}	H_2	0.15×10^3	0.022×10^{-2}
Na	29	5.8	A_1	0.59	0.22
Hg	81	5.2	Ne_1	0.29	0.030
Zn	89	3.7	CCl_4	1.2	8.0
Sn	57	7.3	CS_2	2.6	4.2
Cd	66	5.8	C_6H_6	1.1	5.8
Pb	41	8.8	C_6H_{12}	0.97	8.0
Tl	36	6.7	$C_6H_5NH_2$	2.1	9.9
P_4	2.3	7.7	$C_6H_5NO_2$	1.9	12
S_8	2.5	3.5	$C_6H_4CH_3NH_2$	1.4	9.9
Se_2	4.5	4.0	$C_{10}H_8$	1.1	9.7
Br_2	2.0	3.6	$(C_6H_5)_2NH$	1.4	20
N_2	0.56	0.25	$(C_6H_5CH_2)_2$	1.1	28
O_2	1.5	0.32			

* The unit of pressure is the standard atmosphere and the unit of volume the gram molecular volume of an ideal gas at N.T.P.

The value of the internal pressure for various substances at their melting points (strictly triple points) as given by Eq. (1) is given below. The values for the surface tension have been taken from Fürth's paper (see Table I).

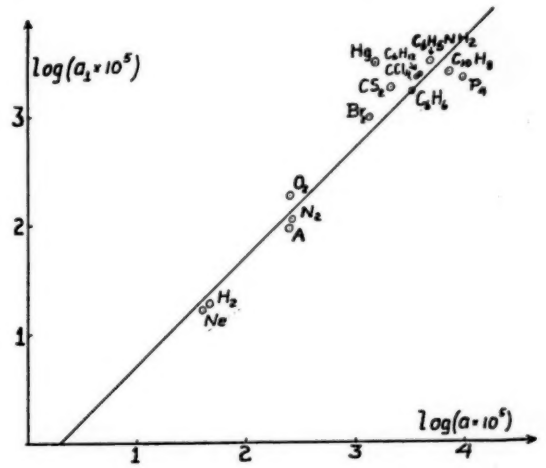

FIG. 1. The abscissae denote the experimental values for van der Waals' constant a and the ordinates the values a_1 obtained from Fürth's theory.

As is well known, the internal pressure p_0 in a liquid is defined as

$$T(\partial p_0/\partial T)_V = T\alpha/\beta, \tag{2}$$

where α is the coefficient of expansion and β is the coefficient of compressibility. If van der Waals' equation be assumed to apply to a liquid, the internal pressure is given by a/V^2 where V is the molecular volume and a is the molecular force term in van der Waals' equation. Thus we have

$$p_0 = a/V^2, \tag{3}$$

and from this it is easily shown that the internal pressure is also equal to the latent heat of vaporization at constant volume per unit volume. The hole theory of the liquid state leads immediately to a connection between van der Waals' a and surface tension σ. This relation is of interest for it was through his studies of surface tension that van der Waals was led to the equation of state. From (1) and (3) we obtain for the van der Waals' force constant

$$a_1 = 1.3\,V^2[\sigma^4/(kT)^4]. \tag{4}$$

It is to be noted that as σ decreases with increasing temperature the value a_1 will decrease with increasing temperature. This is in accordance with observation. In Fig. 1 $\log(10^5 a_1)$ is plotted against $\log(10^5 a)$, a_1 being calculated from the above relation. (The values of a have been taken from *Handbook of Chemistry and Physics*.[3]) It will be observed from Fig. 1 that a is proportional to a_1 and the constant of proportionality is nearly 2.0, whereas the theory requires it to be unity. However, considering the approximate nature of Fürth's model this discrepancy cannot be considered unreasonable.

In a paper to be published shortly we have constructed and solved the Schrödinger equation for a hole in a liquid and determined the eigenvalues of its energy. On this theory we are led to an expression for the intrinsic pressure which does not contain the temperature but only the surface tension and density of the liquid. This gives for the intrinsic pressure the value

$$p_0 = 3.5\sigma(7\pi\sigma/15E)^{\frac{1}{2}},$$

and for the van der Waals' force constant the value

$$a_2 = 3.5\sigma V^2(7\pi\sigma/15E)^{\frac{1}{2}}, \qquad (5)$$

where $E = 3.1h^{4/7}\sigma^{5/7}/\rho^{2/7}$, h being the Planck constant. In Fig. 2 $\log(10^5 a_2)$ has been plotted against $\log(10^5 a)$ and

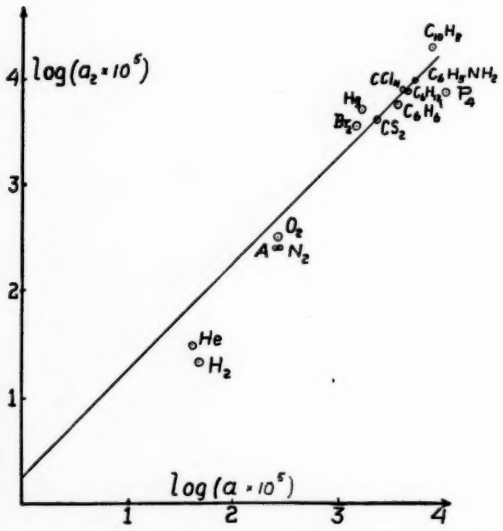

FIG. 2. The abscissae denote the experimental values for van der Waals' constant a and the ordinates the values of a_2 obtained from Eq. (5).

the agreement is satisfactory. The constant of proportionality is again 0.6 instead of being unity.

In the paper referred to above various other applications of the modified hole theory have been discussed, but it is interesting to find that the hole theory leads immediately to a relation between surface tension and van der Waals' constant.

We are very grateful to Dr. Kothari for his kind interest in the work.

[1] Fürth, Proc. Camb. Phil. Soc. **37**, 252 (1941).
[2] See also R. S. Silver, Nature **150**, 605 (1942). It is interesting to note that water passes up through the conduit of trees in a state of tension [Dixon, Proc. Roy. Soc. **B125**, 1 (1938)].
[3] *Handbook of Chemistry and Physics* (Chemical Rubber Publishing Company, Cleveland, 1937–1938), 22nd edition.

Copolymerization of Systems of Three and More Components

T. ALFREY,* *Springfield, Massachusetts*
AND
G. GOLDFINGER,** *Boston, Massachusetts*
May 2, 1944

IN a recent paper[1] these authors have shown that with a steady state assumption the course of copolymerization of a system of two components can be calculated without restricting assumptions as to the relative values of the rate constants involved.

Similarly it is possible to calculate the course of copolymerization of a system of any number of components. This, however, is rather involved because of the great number of rate constants which must be considered. Even the answer to the limited question of the polymer as a function of monomer composition involves $x(x-1)$ rate constant ratios (where x is the number of components). Thus, for a system of three components, A, B, and C, where nine rates of growths are involved, six ratios are required; namely,

$$\alpha^b = k_2^{ab}/k_2^{aa}; \quad \alpha^c = k_2^{ac}/k_2^{aa}; \quad \beta^a = k_2^{ba}/k_2^{bb};$$
$$\beta^c = k_2^{bc}/k_2^{bb}; \quad \gamma^a = k_2^{ca}/k_2^{cc}; \quad \gamma^b = k_2^{cb}/k_2^{cc},$$

where the first upper index denotes the nature of the active group in which the growing chain ends and the second upper index the monomer added in the process. Then the initial polymer composition $a/b/c$ is:

$$\frac{a}{b} = \frac{\beta^a\gamma^b AB + \gamma^a A(\beta^a A + \beta^c C)}{\alpha^b\gamma^a AB + \gamma^b B(\alpha^b B + \alpha^c C)} \cdot \frac{A + \alpha^b B + \alpha^c C}{B + \beta^a A + \beta^c C}, \qquad (1)$$

$$\frac{a}{c} = \frac{\beta^a\gamma^b AB + \gamma^a A(\beta^a A + \beta^c C)}{\alpha^c\beta^a AC + \beta^c C(\alpha^b B + \alpha^c C)} \cdot \frac{A + \alpha^b B + \alpha^c C}{C + \gamma^a A + \gamma^b B}. \qquad (2)$$

Equations (1) and (2) indicate the possibility of predicting the composition of a multipolymer from information gathered from a separate study of each pair of monomers involved. The knowledge of the ratios of the propagation rate constants for each pair of monomers also permits the calculation of the size distribution curve of sequences of units of one kind. This is worth-while information which, in most cases, cannot be obtained otherwise. Thus if the monomer mixture is made up of the monomers A, B, C, $\cdots Y$, the resulting initial copolymer will consist of sequences of a, b, $\cdots$ and y monomer units. The fraction of all a sequences which possess n_a monomer units will be given by a distribution function $N(n_a)$.

$$N(n_a) = \left(\frac{A}{A + \alpha^b B + \alpha^c C + \cdots \alpha^y Y}\right)^{(n-1)} \times \left(1 - \frac{A}{A + \alpha^b B + \alpha^c C + \cdots \alpha^y Y}\right). \qquad (3)$$

In many cases of interest the a sequences will consist mainly of one member—i.e., isolated a units. In other cases relatively long sequences of a's will be present in the copolymer.

* At present at Monsanto Chemical Company, Springfield, Massachusetts.
** At present at Godfrey L. Cabot, Inc., Boston, Massachusetts.
[1] T. Alfrey and G. Goldfinger, J. Chem. Phys. **12**, 205 (1944).